






ARTICLE

Cell type-specific modulation of metabolic, immune-regulatory, and anti-microbial pathways by CD101

Marius Wrage¹, Tim Holland ¹, Björn Nüse¹, Johanna Kaltwasser¹, Jessica Fröhlich¹, Harald Arnold¹, Claudia Gießler¹, Cindy Flamann², Heiko Bruns², Johannes Berges ², Christoph Daniel³, Markus H. Hoffmann^{4,5}, Chakkumkal Anish^{6,7}, Peter H. Seeberger^{6,8}, Christian Bogdan ^{1,9}, Katja Dettmer¹⁰, Manfred Rauh ¹¹ and Jochen Mattner ^{1,9,✉}

© 2024 The Author(s). Published by Elsevier Inc. on behalf of Society for Mucosal Immunology.

This is an open access article under the CC BY-NC-ND license (<http://creativecommons.org/licenses/by-nc-nd/4.0/>).

T lymphocytes and myeloid cells express the immunoglobulin-like glycoprotein cluster of differentiation (CD)101, notably in the gut. Here, we investigated the cell-specific functions of CD101 during dextran sulfate sodium (DSS)-induced colitis and *Salmonella enterica* Typhimurium infection. Similar to conventional CD101^{-/-} mice, animals with a regulatory T cell-specific *Cd101* deletion developed more severe intestinal pathology than littermate controls in both models. While the accumulation of T helper 1 cytokines in a CD101-deficient environment entertained DSS-induced colitis, it impeded the replication of *Salmonella* as revealed by studying CD101^{-/-} x interferon- γ ^{-/-} mice. Moreover, CD101-expressing neutrophils were capable to restrain *Salmonella* infection *in vitro* and *in vivo*. Both cell-intrinsic and -extrinsic mechanisms of CD101 contributed to the control of bacterial growth and spreading. The CD101-dependent containment of *Salmonella* infection required the expression of *Irg-1* and *Nox2* and the production of itaconate and reactive oxygen species. The level of intestinal microbial antigens in the sera of inflammatory bowel disease patients correlated inversely with the expression of CD101 on myeloid cells, which is in line with the suppression of CD101 seen in mice following DSS application or *Salmonella* infection. Thus, depending on the experimental or clinical setting, CD101 helps to limit inflammatory insults or bacterial infections due to cell type-specific modulation of metabolic, immune-regulatory, and anti-microbial pathways.

Mucosal Immunology (2024) 17:892–910; <https://doi.org/10.1016/j.mucimm.2024.06.004>

INTRODUCTION

Dysregulated interactions between microbial or metabolic products and host cells can result in an inadequate generation or function of cellular or humoral components of the innate or adaptive immune system^{1,2}. Alterations of these circuits presumably underlie many immune-mediated and infectious diseases^{1–4}. The detection of these disrupted interrelationships has been challenging. Thus, the identification of biomarkers that reliably indicate alterations in immune responses, metabolic pathways, and disease activities is highly desirable, preferably before tissue pathology manifests. CD101 (IGSF-2, EWI-101, V7) is a promising molecule in this context as its expression changes drastically in immune-mediated disorders and infections^{5,6}.

CD101 belongs to a family of cell-surface immunoglobulin (Ig) superfamily proteins (EWI-2, EWI-3, EWI-F) that share a conserved glutamine-tryptophan-isoleucine (EWI) motif which is not found in other Ig proteins⁷. Memory and regulatory T (Treg)

lymphocytes, granulocytes, monocytes, and dendritic cells (DCs) express CD101^{5,6,8,9}. However, the metabolic and molecular pathways targeted by CD101 in each of these cell subsets have yet to be discovered¹⁰.

Previously, we reported a higher bacterial tissue burden and an exacerbation of immune-mediated organ injury in conventional *Cd101* knockout mice^{5,6,9}. Tissue pathology in these models correlated with an enhanced T cell proliferation and increased interleukin (IL)-17- and interferon (IFN)- γ -production by T lymphocytes. Although CD101-expressing myeloid cells sustained and improved anti-inflammatory Treg function(s) in wild-type litters⁵, the cell-specific function(s) of CD101 on myeloid cell subsets and the functional consequences of the enhanced T helper (Th)1 and Th17 responses in the CD101 knockout are still unknown.

To elucidate the cell-specific functions of CD101 and the molecular and metabolic pathways underlying these functions,

¹Mikrobiologisches Institut-Klinische Mikrobiologie, Immunologie und Hygiene, Universitäts-klinikum Erlangen, Friedrich-Alexander-Universität (FAU) Erlangen-Nürnberg, Erlangen, Germany. ²Medizinische Klinik 5, Universitätsklinikum Erlangen, FAU Erlangen-Nürnberg, Erlangen, Germany. ³Nephropathologische Abteilung, Universitätsklinikum Erlangen, FAU Erlangen-Nürnberg, Erlangen, Germany. ⁴Medizinische Klinik 3, Universitätsklinikum Erlangen, FAU Erlangen-Nürnberg, Erlangen, Germany. ⁵Klinik für Dermatologie, Allergologie und Venerologie, Universitätsklinikum Schleswig-Holstein, Universität zu Lübeck, Lübeck, Germany. ⁶Max Planck Institute of Colloids and Interfaces, Potsdam, Germany. ⁷Bacterial Vaccines Discovery and Early Development, Janssen Pharmaceuticals (Johnson & Johnson), CK Leiden, The Netherlands. ⁸Freie Universität Berlin, Department of Chemistry and Biochemistry, Berlin, Germany. ⁹FAU Profizienz-Zentrum Immunmedizin (FAU I-MED), FAU Erlangen-Nürnberg, Erlangen, Germany. ¹⁰Institut für Funktionelle Genomik, Universität Regensburg, Regensburg, Germany. ¹¹Kinder- und Jugendklinik, Universitätsklinikum Erlangen, FAU Erlangen-Nürnberg, Erlangen, Germany. ✉ email: Jochen.Mattner@uk-erlangen.de

we compared the induction of colitis in conventional and conditional CD101^{-/-} mice before and after application of dextran sulfate sodium (DSS) or infection with *Salmonella enterica subsp. enterica* serotype Typhimurium (*S. Tm*). We observed that Tregs were sufficient for the CD101-mediated protection against experimental colitis in both models. While IFN- γ was the dominant colitogenic cytokine in the DSS model, it contributed to the control of *S. Tm* infection. Moreover, the expression of CD101 on myeloid cells correlated with an increased expression of immune-responsive gene 1 (*Irg-1*) and *Nox2* as well as an enhanced availability of itaconate and reactive oxygen species that were required for limiting bacterial replication and translocation.

RESULTS

DSS application and *S. Tm* infection suppress CD101 expression on neutrophils

Subsets of myeloid cells and T lymphocytes express CD101^{5,6,8,9}, predominantly in the gut¹¹. Here, we investigated the distribution of CD101 on immune cell subsets in different tissues before and after DSS application¹² or *S. Tm* infection¹³ (Supplementary Figs. 1 and 2). We confirmed that primarily immune cells in the lamina propria (LP) and the intestinal epithelium (IE) stained positive for CD101 (Supplementary Fig. 3A). While T lymphocytes represented the majority of CD101-expressing immune cells in the intestine, myeloid cells were the cell type that predominantly expressed CD101 in the bone marrow (BM) (Supplementary Fig. 3B). Following DSS application, the percentage of neutrophils within total LP/IE cells increased in the gut (Figs. 1A and 1B). However, in relation to naive mice, the expression levels of CD101 among neutrophils recovered from intestinal tissues, BM, spleen, and blood were significantly lower following one DSS cycle (Figs. 1C–1E; Supplementary Fig. 3C). Following repetitive DSS cycles, CD101 expression recovered over time and reached expression levels similar to naive mice after the third cycle (Figs. 1C–1E). Thus, despite its local application, DSS induces transient systemic effects on CD101 expression, even on cells in distant tissues.

Relative granulocyte numbers increased also in intestinal tissues, the spleens, or the peritoneal cavity (PC) following oral or systemic *S. Tm* infection (Figs. 1F, 1G, and 1K). We also observed reduced CD101 expression on neutrophils in the IE/LP, the spleen, and the BM or the PC following acute oral or intraperitoneal infections with wild-type *S. Tm* (Figs. 1H–1J, 1L, and 1M). Following oral infection with the attenuated Δ aroA *S. Tm* strain, used to study chronic infections¹⁴, the CD101 expression levels in intestinal tissues within the first days after infection were also lower as compared to naive mice (data not shown). However, the expression of CD101 recovered later on

(Figs. 1H–1J), albeit to a lower extent as compared to the chronic DSS model (Figs. 1C–1E). The overall reduction of CD101 expression on neutrophils in both models was presumably due to the influx of immature neutrophils from the BM into inflamed tissues that have not yet upregulated CD101 and downregulation of CD101 on the cell surface of more mature cells at the site of infection/inflammation^{6,15}.

Neither DSS application nor any *S. Tm* infection route changed CD101-expression on T cells (Supplementary Fig. 4). Following DSS application, the expression of CD101 on CD11b⁺ Ly6G⁻ myeloid cells and CD11b⁺ Ly6C⁺ monocytes did not change while expression levels of CD101 on myeloid cells from the intestine and the spleen were also significantly lower after *S. Tm* infection as compared to naive mice (Supplementary Fig. 3C and Fig. 4). The main cell population that expressed CD101 within CD11b⁺ Ly6G⁻ myeloid cells were CD11b⁺ CD11c⁺ DCs, reflecting the conventional DC2 subset (data not shown). Thus, these data suggest a cell-type specific regulation of CD101 expression in response to inflammatory and infectious insults.

Conventional CD101^{-/-} mice exhibit more severe DSS- and *S. Tm*-induced colitis

To evaluate the course of disease in both colitis models, we exposed CD101^{-/-}, CD101^{+/-}, and CD101^{+/+} littermates to DSS or *S. Tm*. One single course of DSS treatment or repetitive DSS cycles promoted a more severe clinical phenotype in the absence of *Cd101* (Figs. 2A–2F; Supplementary Fig. 5A). While the heterozygous expression of one *Cd101* allele was sufficient to restrain acute DSS colitis (Figs. 2A–2D), both *Cd101* alleles were required to convey an ameliorating effect in chronic DSS colitis (Figs. 2E and 2F).

In chronic *S. Tm* infection, one *Cd101* allele already limited intestinal inflammation (Fig. 2G; Supplementary Fig. 5B). In contrast, during acute infection, we did not detect significant differences between wild-type, CD101^{+/-} and CD101^{-/-} mice (data not shown).

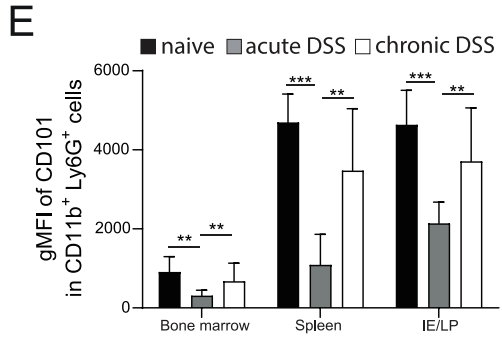
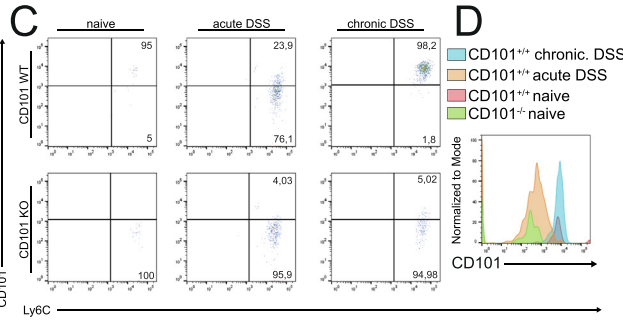
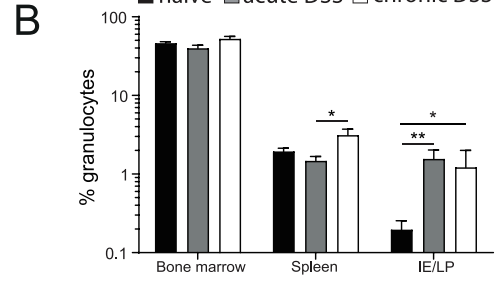
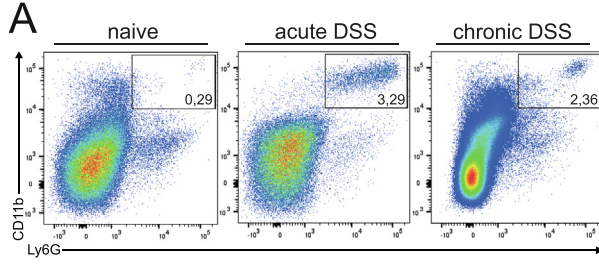
Together, these data demonstrate that *Cd101* exerts mitigating effects in both DSS- and *S. Tm*-induced colitis.

S. Tm replicates and translocates faster in CD101^{-/-} mice

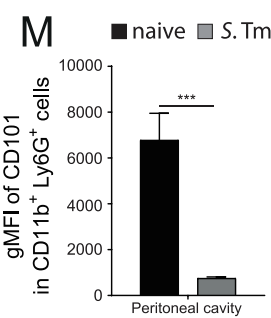
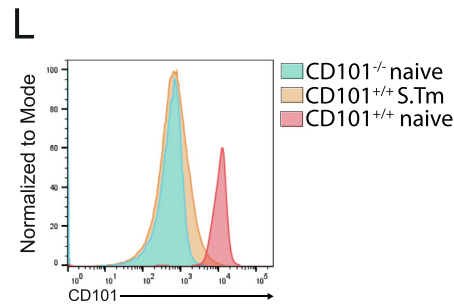
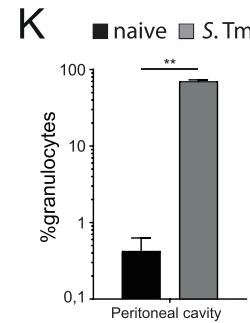
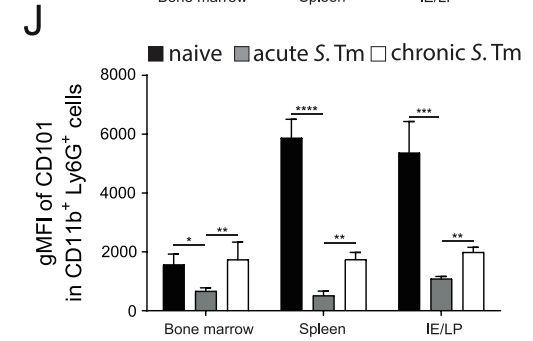
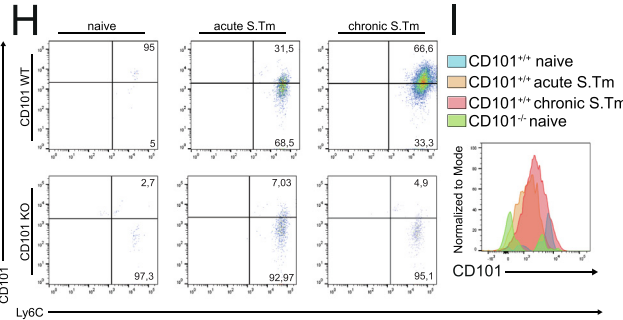
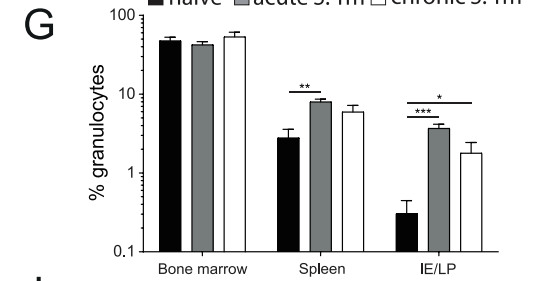
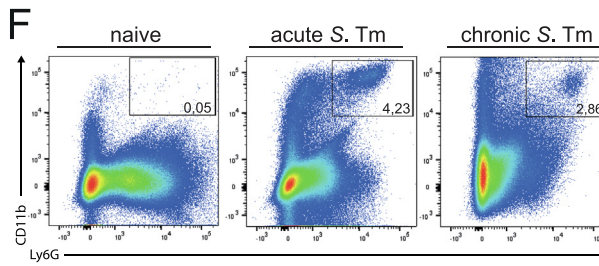
Since CD101^{-/-} mice harbored more bacteria in their tissues compared to controls following infection with certain bacterial species⁶, we assessed whether CD101 also influences the course of *S. Tm* infection. After an acute oral infection with wild-type *S. Tm* or a chronic oral infection with the Δ aroA mutant, we recovered significantly higher numbers of bacterial colony-forming units (CFUs) from the spleens and livers (Fig. 2H) or the feces (Fig. 2I) of CD101^{-/-} mice compared to littermate controls. Inter-

Fig. 1 Mainly neutrophils among myeloid cell subsets become CD101-negative following DSS application or *S. Tm* infection. Three days after one (acute DSS) or three (chronic DSS) DSS cycles (A–E) as well as four (acute *S. Tm*) or 10 days (chronic *S. Tm*) after oral infection (F–J) or 1 day after intraperitoneal infection with *S. Tm* (K–M) the percentages of neutrophils and the geometric mean fluorescence intensities of CD101 were assessed by flow cytometry. Representative FACS dot plots of relative neutrophil numbers from intestinal tissues (A, F) and the expression of CD101 by neutrophils from CD101^{+/+} and CD101^{-/-} mice (C, H) as well as histograms of gMFIs of CD101 (D, I, L) are shown. Summaries of the mean percentages (\pm SD) of relative neutrophil numbers in the indicated organs (B, G, K) and summaries of gMFIs of CD101 (E, J, L) derived from the analysis of 18–20 (A–E), 6–8 (F–J) or 3–8 (K–M) individual mice are depicted. Statistical significance was calculated using analysis of variance with Bonferroni *post hoc* test (* $p \leq 0.05$; ** $p < 0.01$; *** $p < 0.001$; **** $p < 0.0001$). CD = cluster of differentiation; DSS = dextran sulfate sodium; FACS = fluorescence-activated cell sorting; gMFIs = geometric mean fluorescence intensities; IE = intestinal epithelium; LP = lamina propria; *S. Tm* = *Salmonella enterica* Typhimurium; SD = standard deviation.

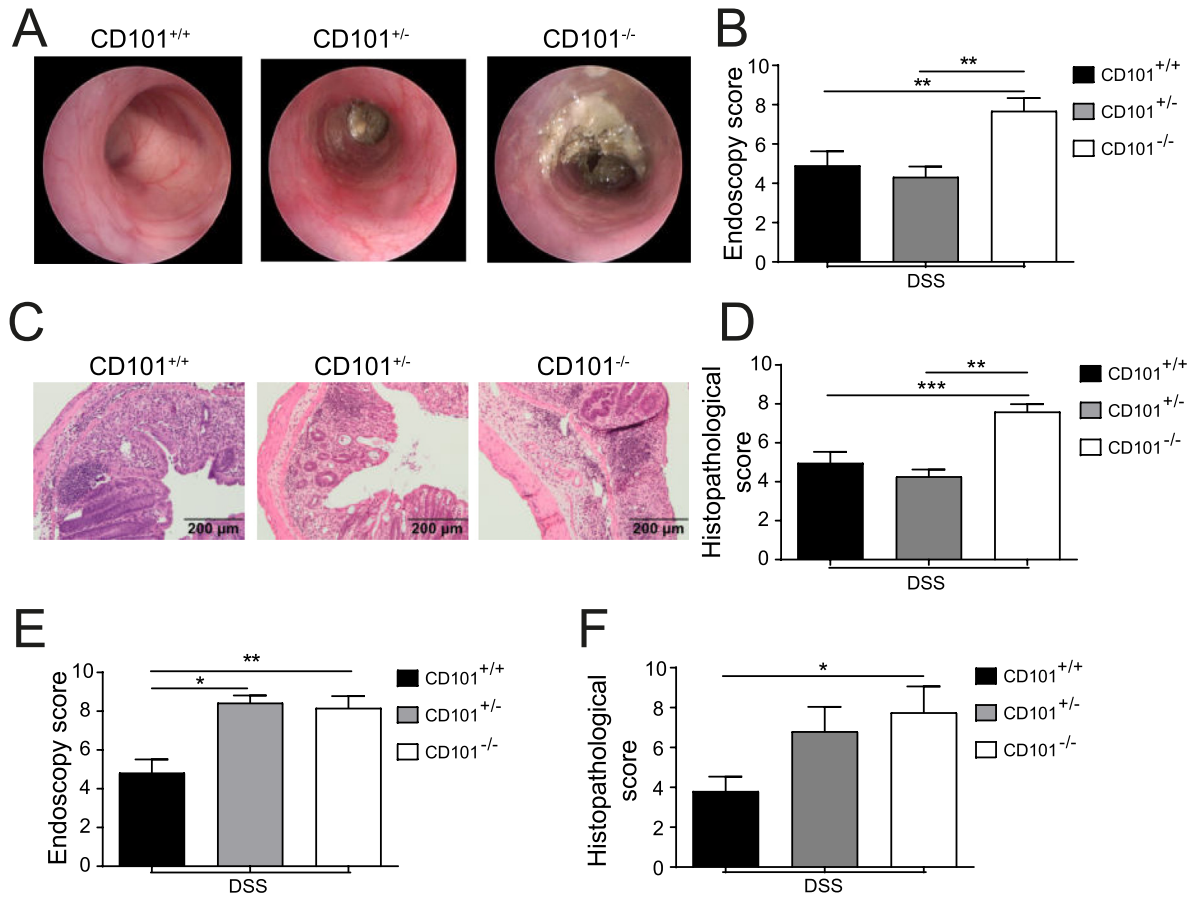
DSS Colitis



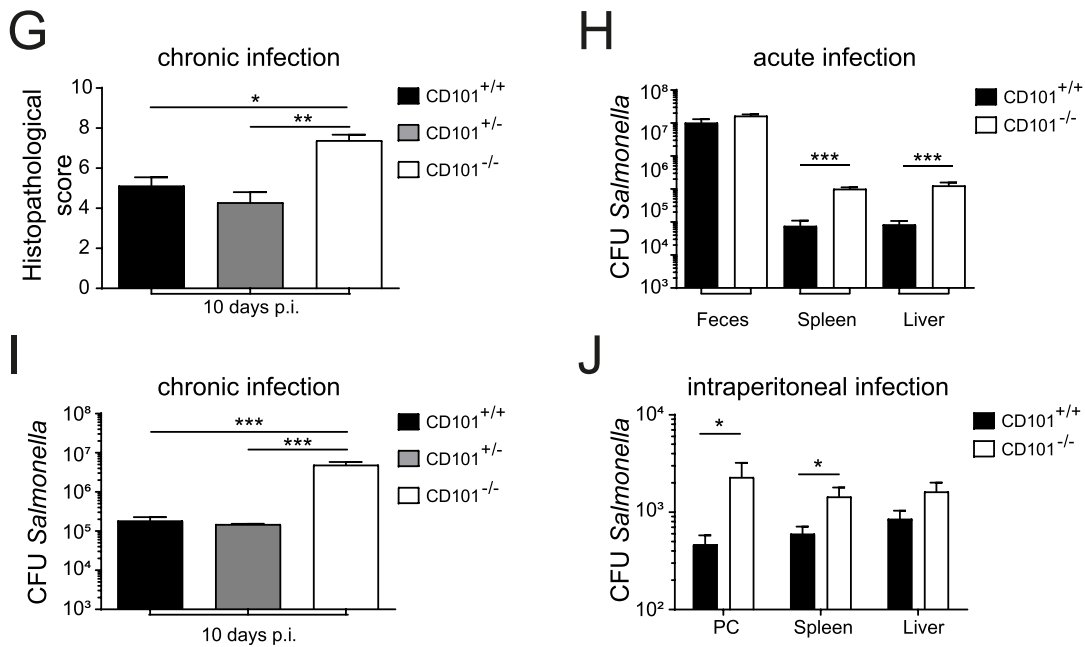
S.Tm infection



DSS Colitis



S.Tm infection



estingly, one *Cd101* allele was sufficient to restrain fecal *S. Tm* replication following chronic infection (Fig. 2I). Furthermore, the expression of CD101 also inhibited the spread of *S. Tm* to the spleen after intraperitoneal inoculation (Fig. 2J). Thus, the expression of CD101 correlates with reduced bacterial replication and spreading during both acute and chronic *S. Tm* infection, independent of the infection route.

Treg-specific *Cd101* is necessary to protect from DSS- and *S. Tm*-induced colitis

To assess the function of CD101 on individual cell subsets on the course of colitis, we crossed different Cre-deleter strains to conditional CD101 knockout (*Cd101^{fl/fl}*) mice⁸. Similar to naive CD101^{-/-} mice, none of the *Cd101^{fl/fl}* strains developed spontaneous colitis (Supplementary Figs. 6A and 6B). However, when subjected to one or repetitive DSS cycles, *Foxp3* Cre x *Cd101^{fl/fl}* mice consistently developed more severe colitis compared to *Cd101^{fl/fl}* controls, *LyzM* Cre x *Cd101^{fl/fl}*, *Cd11c* Cre x *Cd101^{fl/fl}* or *Cx3cr1* Cre x *Cd101^{fl/fl}* mice (Figs. 3A–D; Supplementary Figs. 6C–6E). The kinetics and the extent of CD101 suppression on myeloid subsets that still expressed CD101 in the different conditional *Cd101^{fl/fl}* strains were similar compared to respective wild-type littermates (Supplementary Figs. 7 and 8). Following infection with the *S. Tm* Δ aroA mutant, chronic colitis was more severe in *Foxp3* Cre x *Cd101^{fl/fl}* mice compared to other *Cd101^{fl/fl}* strains and respective wild-type littermate controls (Fig. 3E; Supplementary Figs. 9A and 9B; data not shown). Thus, the expression of CD101 on Tregs, but not on macrophages or dendritic cells is necessary to restrict the inflammation during DSS- and *S. Tm*-induced colitis.

CD101-expressing myeloid cells restrain bacterial infection

To assess the cell-specific influence of CD101 on bacterial replication during acute and chronic infection, we subjected the different conditional *Cd101^{fl/fl}* mice to wild-type (Figs. 3F and 3H) or Δ aroA *S. Tm* (Fig. 3G). *LyzM* Cre x *Cd101^{fl/fl}* mice less efficiently controlled bacterial replication and translocation compared to *Foxp3* Cre x *Cd101^{fl/fl}* mice and littermate controls (Figs. 3F and 3G). Some *LyzM* Cre x *Cd101^{fl/fl}* mice even succumbed to wild-type *S. Tm* infections (Fig. 3H). Since the bacterial burden and the clinical course of infection remained unaltered in *Cd11c* Cre x *Cd101^{fl/fl}* or *Cx3cr1* Cre x *Cd101^{fl/fl}* mice (Supplementary Figs. 9C–9E), CD101-expressing neutrophils most likely account

for the control of bacterial replication and translocation. We also conclude that the limitation of bacterial replication does not inherently contribute to the anti-colitogenic effects mediated by CD101.

Enhanced *Il-17* and *Ifn-g* responses accompany more severe colitis in Treg-specific *Cd101^{fl/fl}* and in conventional CD101^{-/-} mice

To delineate the cellular and molecular pathways underlying the anti-inflammatory and anti-microbial effects mediated by CD101, we assessed the cytokine pattern in intestinal tissues of conventional CD101^{-/-} and conditional *Cd101^{fl/fl}* mice crossed to different Cre-deleter strains. Similar to previous observations in the adoptive T cell transfer model of colitis⁵, the intestinal mucosa of CD101^{-/-} mice exhibited increased copy numbers of *Il-17A* and *Ifn-g* in response to DSS (Figs. 4A and 4B). We also obtained greater *Ifn-g* copy numbers from CD101^{-/-} than from CD101^{+/+} mice following *S. Tm* infection (Fig. 4C). Of note, *Foxp3* Cre x *Cd101^{fl/fl}* mice expressed significantly more *Il-17A* and *Ifn-g* following DSS application (Figs. 4D and 4E) or *S. Tm* infection (Figs. 4F–4H) compared to respective littermate controls. In addition, we observed an increased accumulation of *Il-17F* and *Il-22* in *Foxp3* Cre x *Cd101^{fl/fl}* mice compared to controls following DSS application (Supplementary Figs. 10A and 10B). Interestingly, *LyzM* Cre x *Cd101^{fl/fl}* mice also expressed more *Ifn-g* compared to *Cd101^{fl/fl}* controls upon application of 2.5% DSS (Supplementary Fig. 10C), a DSS concentration that *Foxp3* Cre x *Cd101^{fl/fl}* mice did not tolerate anymore. Nonetheless, CD101 deficiency on Tregs is primarily associated with enhanced Th1 and Th17 responses.

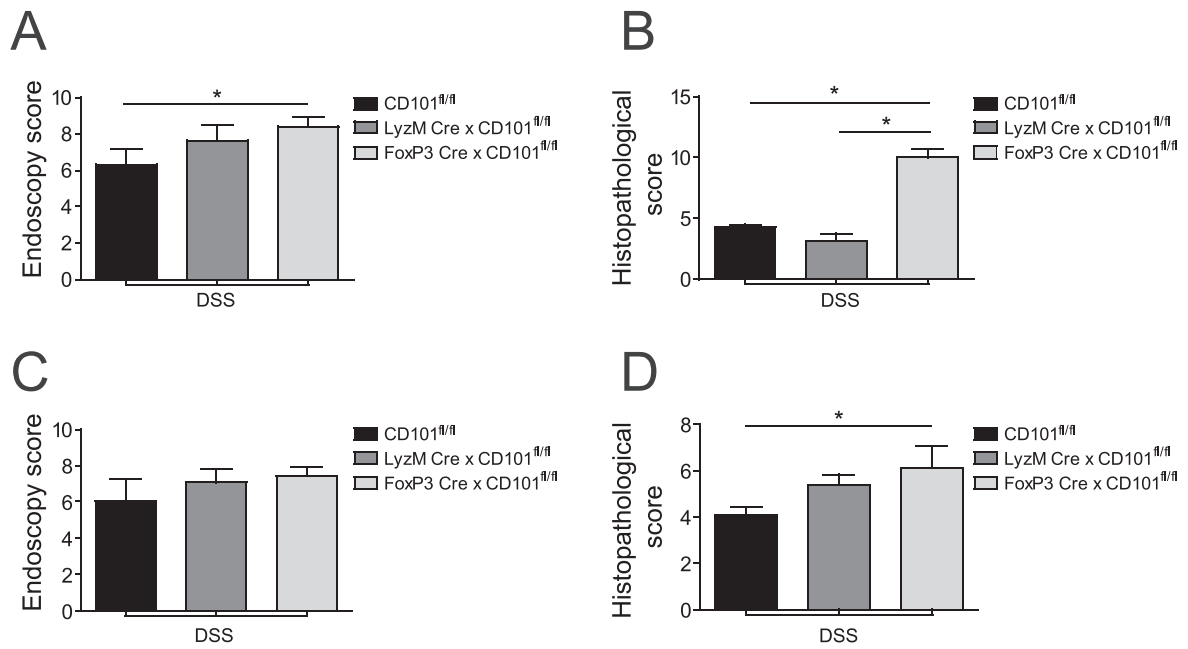
In addition to the heightened levels of IL-17 and IFN-g, we detected significantly less IL-10 in the intestinal mucosa of CD101^{-/-} mice (Supplementary Fig. 10D). Vice versa, *Foxp3* Cre x *Cd101^{fl/fl}* mice contained more IL-10 in the gut, particularly following chronic colitis, compared to *LyzM* Cre x *Cd101^{fl/fl}* mice and littermate controls (Supplementary Fig. 10E).

Deletion of IFN-g in CD101^{-/-} mice reverts DSS colitis but promotes *S. Tm* infection

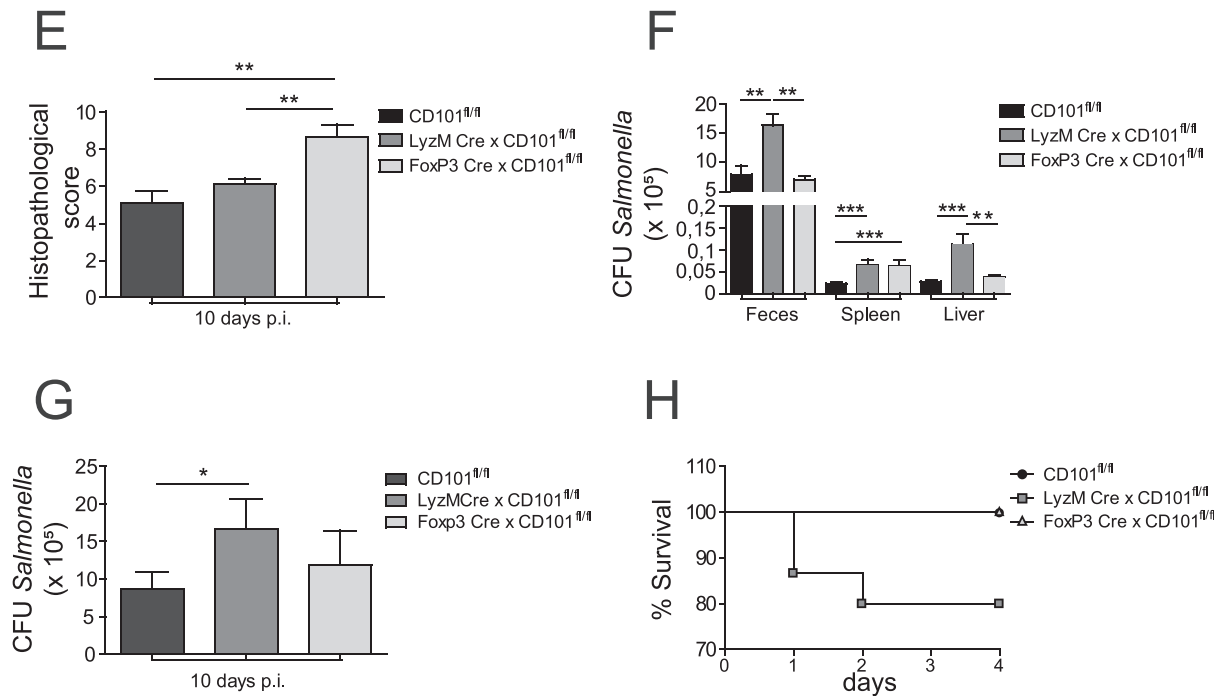
Next, we assessed the impact of the cytokines regulated in a CD101-dependent manner on colitis progression. As CD101 expression and IL-10 production correlate with protection from disease⁵ and as IL-10^{-/-} or IL-10R^{-/-} mice already spontaneously

Fig. 2 The expression of CD101 on myeloid cells and T lymphocytes protects from DSS- and *S. Tm*-induced colitis and contributes to the control of bacterial infection. (A–F) The induction of intestinal inflammation in CD101^{+/+}, CD101^{+/-} and CD101^{-/-} littermates was monitored by high-resolution endoscopy (A, B, E) or histopathological analysis of H&E-stained tissue sections (C, D, F) 10 (A–D) and 52 (E, F) days after DSS application. Representative images from colonoscopies (A) or from H&E-stained tissue sections (\bar{c} = 500 $\mu\text{m}>$). (C) as well as the means \pm SD of the endoscopic (B, E) and histopathologic scores (D, F) from 19 CD101^{+/+}, 14 CD101^{+/-} and 33 CD101^{-/-} mice (B, D) or from 12 CD101^{+/+}, 11 CD101^{+/-} and 16 CD101^{-/-} mice (E, F) are displayed. Statistical significance was calculated using a Kruskal-Wallis test (* $p \leq 0.05$; ** $p < 0.01$; *** $p < 0.001$). (G) The induction of intestinal inflammation in six CD101^{+/+}, 5 CD101^{+/-} and 10 CD101^{-/-} littermates was monitored by histopathological analysis of H&E-stained tissue sections 10 days after oral infection with *S. Tm* Δ aroA. The means \pm SD of the histopathological scores are displayed. Statistical significance was calculated using a Kruskal-Wallis test (* $p \leq 0.05$; ** $p < 0.01$). (H–J) The bacterial burden in the indicated organs (H, J) or in the feces (I) from individual CD101^{+/+}, CD101^{+/-} and CD101^{-/-} mice on day 4 (H) and day 10 (I) after oral infection with wild-type (H) and Δ aroA *S. Tm* (I) or day 2 (J) after intraperitoneal infection with wild-type *S. Tm* was assessed by CFU plating assay and limiting dilution. Each bar represents the mean \pm SD of 9–15 (H), 13–24 (I) or 12–15 (J) individual mice per group. Statistical significance was calculated using a Kruskal-Wallis test comparing bacterial load in each organ (* $p \leq 0.05$; *** $p < 0.001$). CD = cluster of differentiation; CFU = colony forming unit; Δ aroA = *S. Tm* mutant strain that lacks the *aroA* encoding 5-enolpyruvyl-3-phosphoshikimate synthetase; H&E = hematoxylin and eosin; PC = peritoneal cavity; SD = standard deviation.

DSS Colitis



S.Tm infection



develop severe colitis^{16,17}, we refrained from crossing either strain to CD101^{-/-} mice, because an even more severe clinical phenotype in respective double knockouts was to be expected. Since IFN-g and Th17 mRNA levels increased in CD101^{-/-} mice (Fig. 4), we tested whether the additional deletion of either one of these two cytokines in CD101^{-/-} mice ameliorated the course of colitis by crossing conventional CD101^{-/-} mice to IFN-g^{-/-} and IL-17A/F^{-/-} mice¹⁸. The role of IL-17 in the pathogenesis of colitis remains controversial, with IL-17A and IL-17F exerting opposite effects on the course of colitis¹⁹. Since both cytokines accumulated in colitic tissues of CD101-deficient mice, we utilized IL-17A/F^{-/-} mice¹⁸. In accordance with previous observations^{20,21}, neither IL-17A nor IL-17F signaling influenced the course of *S. Tm* colitis (data not shown). Deletion of IL-17A/F in CD101^{-/-} mice also had no significant impact on the progression of DSS colitis (Fig. 5A). In contrast, IFN-g^{-/-} x CD101^{-/-} mice developed clinically and histopathologically milder colitis compared to CD101^{-/-} littermates following DSS application and lost significantly less weight (Figs. 5B–5D). Thus, IFN-g rather than Th17 cytokines promote intestinal pathology in the DSS colitis model.

In *S. Tm*-induced colitis, IFN-g was pivotal for anti-bacterial defense as evidenced by an enhanced accumulation of *S. Tm* in the feces of IFN-g^{-/-} x CD101^{-/-} mice and an increased translocation of *S. Tm* in both, IFN-g^{-/-} and IFN-g^{-/-} x CD101^{-/-} mice (Figs. 5E–5G). Compared to the DSS model, the additional deletion of IFN-g in CD101^{-/-} mice less significantly affected wasting disease and the severity of colitis following *S. Tm* infection (data not shown). Thus, the IFN-g-dominated immune response in CD101^{-/-} mice underlies the induction of severe colitis in the DSS model, but contributes to the control of bacterial infection rather than to intestinal pathology in the *S. Tm* model.

The expression of CD101 is associated with the phagocytic and anti-bacterial activity of neutrophils

CD101 is pivotal for Tregs to restrict intestinal pathology (Figs. 3A–3E), but at the same time promotes anti-bacterial activity of myeloid cells (Figs. 3F–3H). Since *LyzM* Cre deletes *Cd101* in macrophages and neutrophils, but not in DCs (Supplementary Fig. 7; data not shown), we investigated the contribution of macrophages and neutrophils to anti-microbial defense in more detail. Neutrophils, but not macrophages, from CD101^{-/-} and *LyzM* Cre x *Cd101^{fl/fl}* mice phagocytosed more slowly and fewer numbers of *E. coli*- and *Staphylococcus aureus*-labeled bioparticles and of pH-sensitive, fluorogenic dye-conjugates compared to their CD101-expressing counterparts (Figs. 6A–6D; Supplementary Figs. 11A–11C; data not shown). Furthermore, neu-

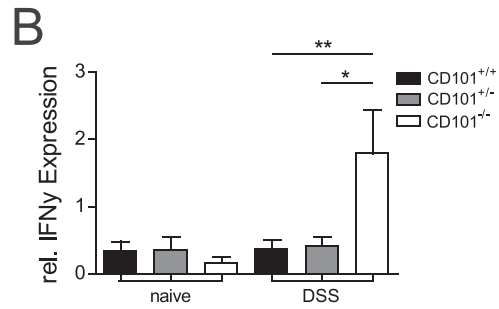
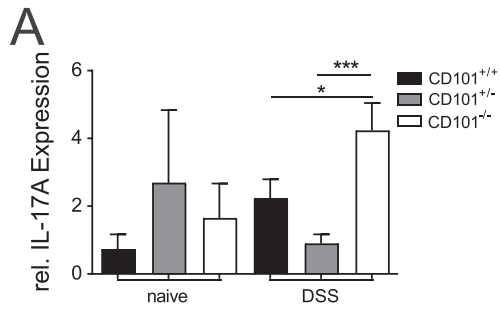
trophils from CD101^{+/+} compared to CD101^{-/-} mice eliminated *S. Tm* faster in gentamicin protection assays (Fig. 6E). Importantly, flow cytometry of mixed CD45.1⁺CD101⁺/CD45.1⁻CD101⁻ BM chimeras, that were infected with GFP-labeled *S. Tm*, revealed that fewer GFP-positive events were detected in neutrophils within the CD101^{-/-} compartment as compared to neutrophils of the CD101^{+/+} compartment (Fig. 6F). In macrophages, CD101 exhibited less striking effects on bacterial uptake and replication than in neutrophils (Fig. 6F; Supplementary Fig. 11D). Moreover, the expression of the inducible or type 2 nitric oxide synthase *Nos2*, which has major anti-microbial effects²², was comparable between CD101^{+/+} and CD101^{-/-} macrophages (Supplementary Fig. 11E). Thus, the more efficient control of bacterial infections in CD101-expressing mice predominantly correlates with an improved anti-microbial and phagocytic activity of neutrophils.

To assess the pathways underlying the improved infection control in wild-type neutrophils, we performed qPCRs on genes involved in phagocytosis and bacterial killing. Interestingly, mRNA copy numbers of *Irf-5*, which is associated with the ability of neutrophils to phagocytose bacteria²³, accumulated faster in CD101-expressing phagocytes than in neutrophils from CD101^{-/-} mice upon exposure to *S. Tm* *in vitro* (Supplementary Fig. 11F). In contrast, *Irf-5* mRNA levels did not significantly differ between immune cell preparations isolated from the intestines of *S. Tm*-infected or DSS-treated CD101^{+/+} versus CD101^{-/-} mice (data not shown). Although IRF-5 was reported to regulate TLR-mediated pro-inflammatory cytokine production²³, we did not detect significant differences in *Tnf* and *Il-1β* as well as *Tlr2*, *Tlr4*, and *Tlr9* copy numbers in neutrophils purified from the gut of CD101^{+/+} and CD101^{-/-} mice (Supplementary Figs. 12A–12E; data not shown). Accordingly, the mRNA levels of *Runx1*, which has been linked to inflammatory cytokine release²⁴, were only slightly and inconsistently reduced in intestinal tissue-derived neutrophils of CD101^{-/-} mice (Supplementary Fig. 12F). Moreover, neutrophils from CD101^{+/+} and CD101^{-/-} mice showed a similar expression of Sca-1, a hematopoietic marker previously detected on immature neutrophils with high pathogenic potential²⁵ (Supplementary Figs. 12G and 12H), confirming that CD101 does not primarily influence the inflammatory phenotype of neutrophils. Finally, CD101 did not affect neutrophil survival (Supplementary Figs. 12I and 12J).

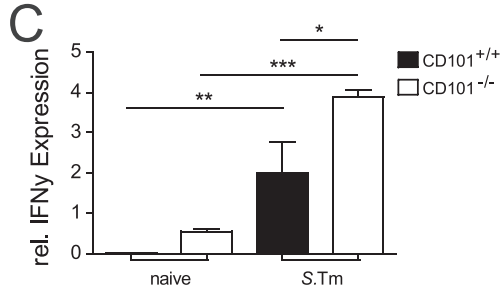
Next, we studied the phagocyte nicotinamide adenine dinucleotide phosphate (NADPH)-oxidase (phox or NOX2) which generates reactive oxygen species (ROS) and substantially contributes to anti-microbial defense²⁶. Similar to *Irf-5*, *S. Tm* more

Fig. 3 CD101 expressing Tregs are sufficient to ameliorate DSS- and *S. Tm*-induced colitis. (A–E) The induction of intestinal inflammation in the indicated mouse strains was monitored by high-resolution endoscopy (A, C) and histopathological analysis of H&E-stained tissue sections (B, D, E) 10 (A, B) and 52 (C, D) days after DSS application or 10 days (E) after infection with ΔaroA *S. Tm*. The means ± SD of the endoscopic and histological scores from 6–7 individual mice are displayed. Statistical significance was calculated using a Kruskal-Wallis test (***p* < 0.01). Error bars indicate the SD of the mean. (F, G) The bacterial burden in the indicated organs on day 4 post infection with wild-type *S. Tm* (F) and in the feces on day 10 post infection with ΔaroA *S. Tm* (G) of the indicated mouse strains was assessed by CFU plating assay and limiting dilution. Each bar represents the mean ± SD of 12–17 individual mice per group. Statistical significance was calculated using a Kruskal-Wallis test (***p* < 0.01; ****p* < 0.001) comparing bacterial load in each organ. (H) Kaplan-Meier survival curves were plotted for 14 individual *Cd101^{fl/fl}* littermate controls, 12 *LyzM* Cre x *Cd101^{fl/fl}* and six *Foxp3* Cre x *Cd101^{fl/fl}* mice following infection with wild-type *S. Tm*. Statistical significance was determined by log-rank test. CD = cluster of differentiation; CFU = colony forming unit; ΔaroA = *S. Tm* mutant strain that lacks the *aroA* encoding 5-enolpyruvyl-3-phosphoshikimate synthetase; DSS = dextran sulfate sodium; H&E = hematoxylin and eosin; Treg = regulatory T cell; *S. Tm* = *Salmonella enterica* Typhimurium; SD = standard deviation.

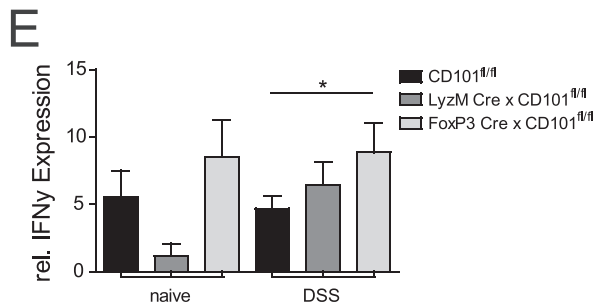
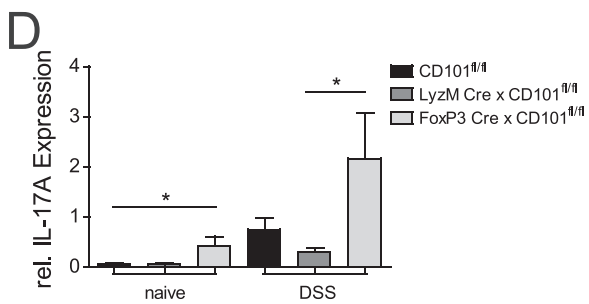
DSS Colitis



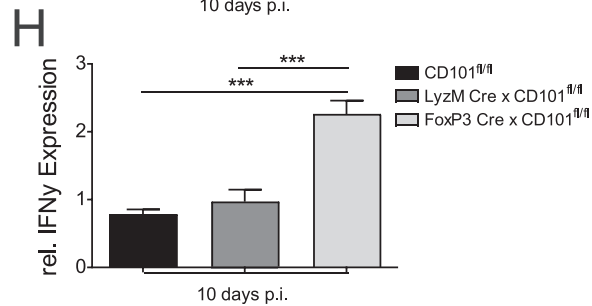
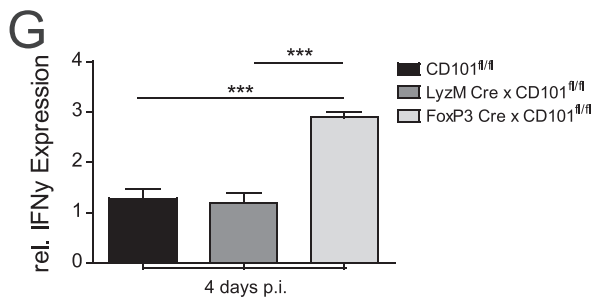
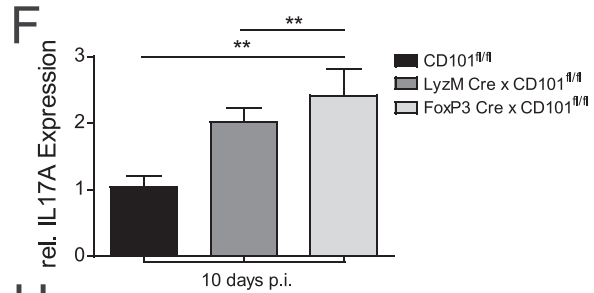
S.Tm infection



DSS Colitis



S.Tm infection



rapidly induced *Nox2* expression and the release of ROS in neutrophils from CD101^{+/+} compared to neutrophils from CD101^{-/-} mice (Figs. 6G and 6H). Neutrophils isolated from the LP of CD101^{+/+} mice expressed higher levels of *Nox2* mRNA than samples from CD101^{-/-} mice following *S. Tm* infection (Fig. 6I). Furthermore, we detected significantly more *Nox2* copy numbers in neutrophils purified from intestinal tissues of *Foxp3* Cre x *Cd101*^{fl/fl} mice compared to neutrophils derived from *LyzM* Cre x *Cd101*^{fl/fl} mice and *Cd101*^{fl/fl} mice (Fig. 6j). In contrast to the *S. Tm* infection model, DSS colitis did not alter *Nox2* expression in a CD101-dependent manner (data not shown).

Together, these data directly link the expression of CD101 in the myeloid compartment to an improved capacity of neutrophils to take up *Salmonella*, produce ROS, and kill the phagocytosed bacteria.

CD101 expression on neutrophils promotes *Irg1*-mediated production of itaconate

Recognition of invading bacteria by neutrophils disrupts the tricarboxylic acid (TCA) cycle, which shifts host metabolism from oxidative phosphorylation toward aerobic glycolysis. To generate NADPH that is required for ROS production by NOX2, neutrophils not only use glycolysis but also employ the pentose-phosphate-pathway as well as glutaminolysis (to degrade glutamine to the TCA intermediates alpha-ketoglutarate and malate) and the citrate-malate-pyruvate cycle²⁷. To assess the impact of CD101 on neutrophils on these metabolic processes, we purified neutrophils from *S. Tm*-infected CD101^{+/+} and CD101^{-/-} mice and determined the respective metabolic intermediates by high performance liquid chromatography electrospray ionization mass spectrometry/mass spectrometry (HPLC-ESI-MS/MS) or hyphenated mass spectrometry. Pyruvate, the final product of aerobic glycolysis, accumulated in higher concentrations in neutrophils from CD101^{-/-} mice (Fig. 7A). In contrast, concentrations of lactate, the end product of anaerobic glycolysis were similar between neutrophil lysates from both mouse strains (Supplementary Fig. 13A), suggesting that enhanced aerobic glycolysis is required in CD101^{-/-} neutrophils compared to CD101^{+/+} neutrophils. Since pyruvate fuels the TCA cycle as precursor, some TCA intermediates such as alpha-ketoglutarate, fumarate, and malate also accumulated in higher concentrations in neutrophils from CD101^{-/-} mice compared to neutrophils from CD101^{+/+} mice (Figs. 7B–7D). Furthermore, the accumulation of alpha-ketoglutarate and malate might reflect a compensatory attempt of CD101-deficient neutrophils to generate ROS²⁸ for the insufficient expression of *Nox2* in intestinal tissues following *S. Tm*

infection. Indeed, the accumulation of aspartate (asp) was significantly higher in CD101^{-/-} neutrophils compared to CD101^{+/+} neutrophils (Supplementary Fig. 13B). In contrast, concentrations of citrate and succinate (Supplementary Figs. 13C and 13D), two TCA intermediates that have been associated with inflammation^{29,30} and the induction of virulence genes in *S. Tm*³¹, were not significantly different between CD101^{-/-} and CD101^{+/+} neutrophils. Accordingly, the expression of the succinate dehydrogenase (*Sdh*) that is inhibited by citrate²⁹, was comparable in neutrophils from CD101^{-/-} mice compared to littermate controls (Supplementary Figs. 13E and 13F). Moreover, CD101-deficiency did not affect neutrophil extracellular traps and neutrophil extracellular trap formation or the expression of integral enzymes of the mitochondrial electron transport chain such as *Sdh*³² (Supplementary Fig. 14 and data not shown).

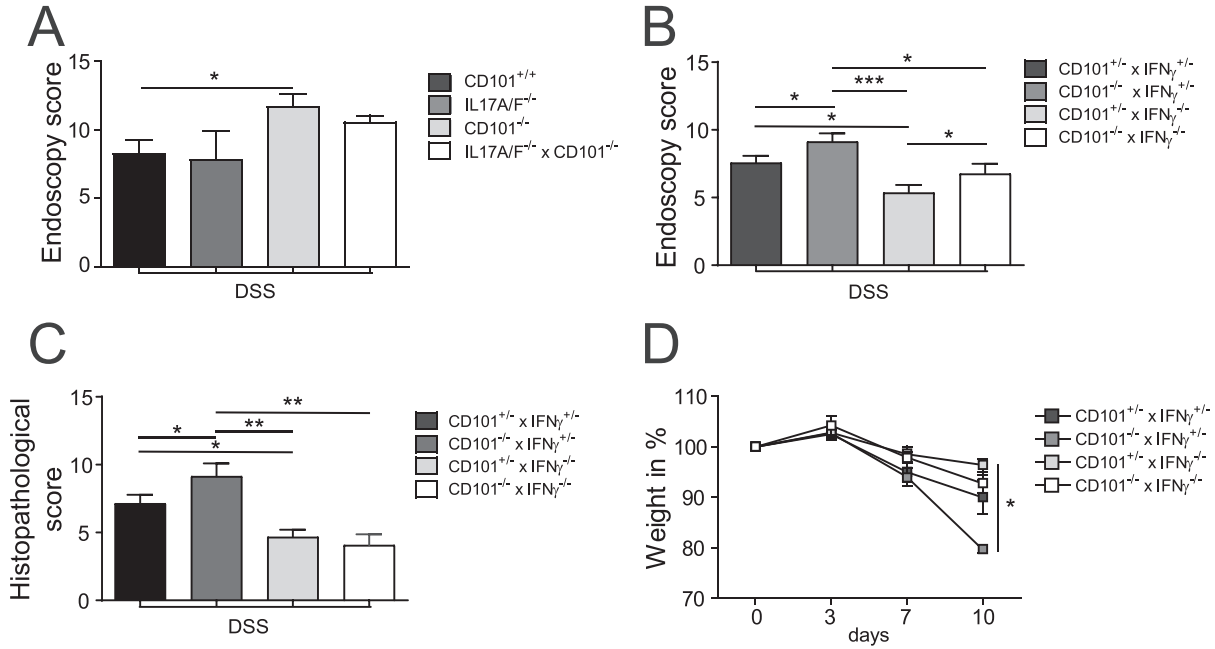
The immune-responsive gene 1 *Irg1* encodes the mitochondrial enzyme IRG1 [also termed aconitate decarboxylase 1 (ACOD1)], which catabolizes the conversion of the TCA cycle intermediate cis-aconitate into itaconate^{33,34}. Itaconate exhibits potent anti-inflammatory and anti-microbial properties³⁵, partly due to the modulation of ROS³⁶. Furthermore, itaconate modifies and inhibits key glycolytic enzymes^{37,38}. Since *Irg-1* is strongly upregulated in phagocytes under pro-inflammatory conditions or upon infection³⁹, we assessed the expression of *Irg-1* and the accumulation of itaconate in neutrophils and different tissues. The expression of *Irg-1* was significantly enhanced in neutrophils purified from intestinal tissues of CD101^{+/+} compared to CD101^{+/-} and CD101^{-/-} litters following *S. Tm* infection (Fig. 7E). *Foxp3* Cre x *Cd101*^{fl/fl} mice that still express CD101 on myeloid cells, also exhibited an enhanced expression of *Irg-1* in the gut upon infection (Fig. 7F). In contrast, *LyzM* Cre x *Cd101*^{fl/fl} mice failed to induce *Irg-1* in both models, linking the expression of CD101 on myeloid cells to the upregulation of IRG-1. In line with these results, we detected an increase of *Irg-1* in neutrophils that were purified from naive CD101^{+/+} mice and exposed to *S. Tm* *in vitro* (Fig. 7G). In neutrophils that were recovered from the PC of CD101^{+/+} mice 1 day after intraperitoneally (i.p.) injection of *S. Tm*, higher concentrations of itaconate, the product of IRG1, were present than in neutrophils taken from infected CD101^{-/-} mice (Fig. 7H). The lack of itaconate might contribute to the insufficient control of bacterial replication and/or enhanced inflammation in CD101^{-/-} mice.

Irg-1 and *Nox2* underlie the CD101-mediated protection from *S. Tm* infection

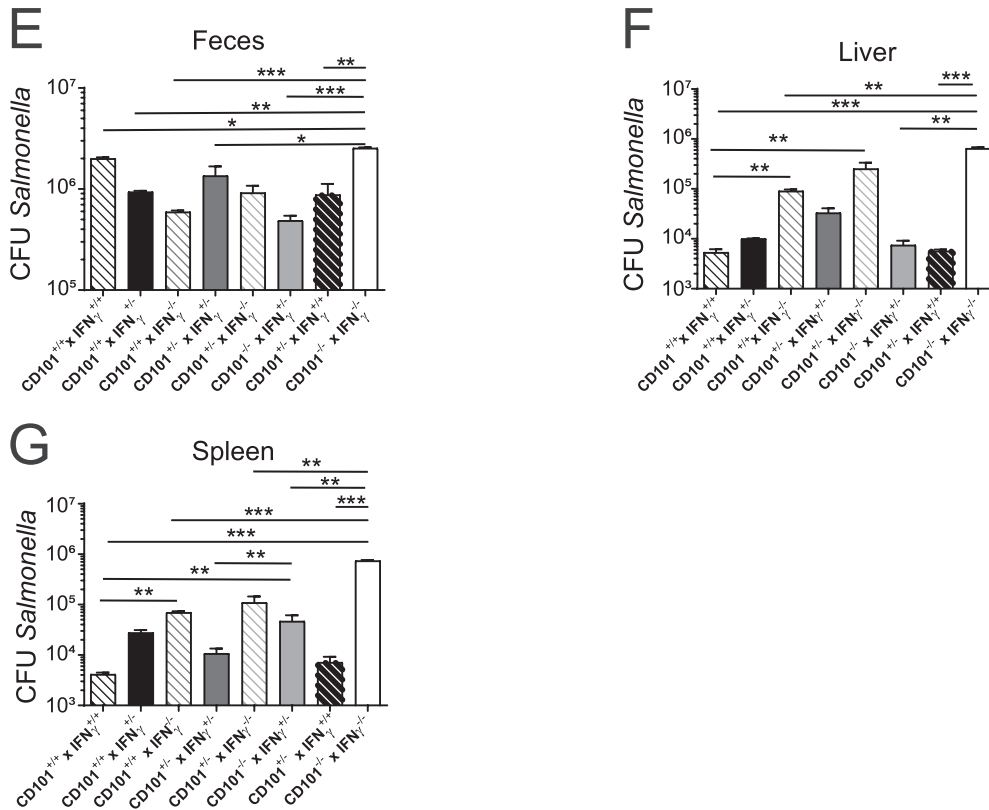
Irg-1-dependent production of itaconate has been reported to exert various immunomodulatory activities, including the regu-

Fig. 4 A Treg-specific knockout of *Cd101* enhances, similarly as a conventional *Cd101* knockout, Th1 and Th17 responses during experimental colitis. (A–C) *Il-17A* (A) and *Ifn-g* (B, C) mRNA copies were determined by RT-qPCR in CD45⁺ CD3⁺ cells isolated from colonic tissues of seven CD101^{-/-} (A, B) or six CD101^{-/-} mice (c) and respective CD101^{+/-} and CD101^{+/+} littermate controls, treated with one DSS cycle (A, B) or infected orally with Δ aroA *S. Tm* for 10 days (c), respectively. (D–G) *Il-17A* (D, F) and *Ifn-g* (E, G, H) mRNA copies were analyzed by RT-qPCR in nine (D, E) or 4–6 (F–H) *Foxp3* Cre x *CD101*^{fl/fl} mice or *LyzM* Cre x *CD101*^{fl/fl} mice and respective controls, treated with one DSS cycle (D, E) or infected orally for 4 (G) or 10 days (F, H) with wild-type or Δ aroA *S. Tm*. The ratio of the mRNA copies of the indicated genes relative to the *Hprt* copies was calculated, and the relative increase in the respective gene copy numbers was displayed. Data were analyzed using the Kruskal-Wallis test followed by Dunn's *post hoc* test (A, E), one-way ANOVA followed by Bonferroni's *post hoc* test (B, D, F–H) or a Mann-Whitney U test (C) (**p* ≤ 0.05; ***p* < 0.01; ****p* < 0.001). Error bars indicate SD of the mean. ANOVA = analysis of variance; CD = cluster of differentiation; Δ aroA = *S. Tm* mutant strain that lacks the *aroA* encoding 5-enolpyruvyl-3-phosphoshikimate synthetase; DSS = dextran sulfate sodium; IFN = interferon; IL = interleukin; mRNA = messenger ribonucleic acid; RT-qPCR = reverse transcription quantitative polymerase chain reaction; *S. Tm* = *Salmonella enterica* Typhimurium; Th = T helper cell; Treg = regulatory T cell.

DSS Colitis



S.Tm infection



lation of phagocyte NOX2⁴⁰. NOX2 generates ROS⁴¹, which not only contribute to anti-microbial defense⁴², but also promote the progression of experimental colitis and the exacerbation of human inflammatory bowel disease (IBD)^{43–45}. As CD101 expression enhanced both *Irg-1* and *Nox2* expression and activity (Figs. 6E–6H and 7E–7H), we crossed CD101^{-/-} mice to IRG1^{-/-} animals and to a mouse strain with a spontaneous mutation in the *neutrophil cytosolic factor 1* (*Ncf1*) gene, which encodes the 47kDa subunit (p47^{phox} or NCF1) of NOX2⁴⁶. Surprisingly, IRG1^{-/-} x CD101^{-/-} mice controlled bacterial infection and translocation less efficiently compared to IRG1^{-/-} or CD101^{-/-} litters and wild-type controls (Figs. 8A–8C). The inefficient control of bacterial infection in IRG-1 x CD101-double-deficient mice was associated with a decreased *Nox2* expression and ROS production compared to CD101^{-/-} littermates (Fig. 8D; data not shown). In line with this finding, all *Ncf-1*^{-/-} x CD101^{-/-} mice succumbed to *S. Tm* infections, similar to *Ncf-1*^{-/-} mice (Fig. 8E). *S. Tm* replicated and translocated faster in *Ncf-1*^{+/-} x CD101^{+/-} than in *Ncf-1*^{+/+} x CD101^{+/-} mice, while *Ncf-1*^{+/-} x CD101^{-/-} littermates were most susceptible (Figs. 8F–8H). Thus, CD101 promotes anti-microbial *Irg-1* and *Nox2* expression and activity. Conversely, *Irg1*^{-/-} and *Ncf-1*^{-/-} mice exhibited a similar CD101 expression compared to the respective wild-type litters (Supplementary Fig. 15). Moreover, intestinal pathology following *S. Tm* infection or DSS application was similarly severe in *Irg-1*^{-/-} x CD101^{-/-} mice and *Ncf-1*^{+/-} x CD101^{-/-} mice compared to respective CD101^{-/-} littermates (data not shown). The lack of a colitis phenotype in both double-deficient mouse lines is also in accordance with the comparable severity of colitis seen in *LyzM* Cre x *Cd101*^{fl/fl} mice and littermate controls. Thus, the *Cd101*- and *Irg-1*-mediated promotion of *Nox2* expression and activity is critical for the control of bacterial infection by neutrophils without affecting the severity of inflammation.

CD101 expression on myeloid cells correlates inversely with serum reactivity to intestinal microbial antigens in IBD patients

Recently, we reported that the expression of CD101 on myeloid cells and T lymphocytes correlates inversely with disease severity in IBD patients⁵. Since IBD patients exhibit compromised intestinal barrier integrity⁴⁷ and myeloid cells lose CD101 expression following microbial exposure⁶, we tested, whether increased systemic dissemination of microbial antigens might contribute to the suppression of CD101 expression on myeloid cells in IBD patients. Therefore, we assessed the presence of antibodies in the sera of IBD patients that recognize oligosaccharides resembling cell wall structures of fungi and bacteria

commonly found in the intestinal microbiome⁴⁸. Patients with a lower expression of CD101 on peripheral myeloid cells exhibited a greater reactivity to yeast cell mannans or to oligosaccharides of intestinal bacteria compared to patients that have greater numbers of CD101-expressing immune cells, as displayed by the increased fluorescence intensities (Figs. 9A–9C).

CD101 sustains *Nox2* and *Irg1* expression in human myeloid cells

Despite the loss of CD101 surface expression following DSS application or bacterial infection (Fig. 1), *Cd101* promotes and sustains *Irg1* and *Nox2* copy numbers in intestinal tissues of mice and in murine myeloid cells (Figs. 6 and 7). To substantiate and translate these findings, we compared the expression of *Irg1* and *Nox2* in human peripheral blood neutrophils before and after stimulation with heat-killed *E. coli*. Microbial exposure correlated in humans with a reduced CD101 expression on myeloid cells, but not on T cells (Figs. 9D and 9E), and mirrors the situation observed in mice⁶. As the number of CD101-positive myeloid cells and T lymphocytes was donor-dependent, we grouped these donors into CD101^{high} and CD101^{low} cohorts and compared the number of *Nox2* and *Irg1* copies between both cohorts. Copy numbers of *Nox2* and *Irg1* among unstimulated myeloid cells from CD101^{high} and CD101^{low} donors did not differ significantly (Figs. 9F and 9G). Following stimulation with heat-killed *E. coli*, however, individuals with a higher initial CD101 expression on myeloid cells still contained more copy numbers of *Nox2* than individuals with a lower expression (Fig. 9F), although overall *Nox2* copy numbers decreased with CD101 expression. *Irg1* expression increased following bacterial stimulation (Fig. 9G), particularly in the cohort with high CD101 expression on myeloid cells. Thus, *Cd101* sustains *Irg-1* and *Nox2* in humans similarly as in mice.

DISCUSSION

Using conventional CD101^{-/-} and conditional *Cd101*^{fl/fl} mice in combination with functional, transcriptional and metabolome analyses, our data link CD101 expression to cell type-specific immune functions. Thereby we identified neutrophils and Tregs as the two cell populations through which CD101 mediates its anti-inflammatory and anti-microbial effects (Supplementary Fig. 16). While CD101-expressing Tregs were necessary to restrict DSS- and *S. Tm*-induced colitis due to the suppression of IFN- γ production, a hampered release of IFN- γ also fostered *S. Tm* infection. Moreover, CD101 promoted the antimicrobial activity of neutrophils, thereby limiting bacterial replication and systemic spread during *S. Tm* infection. Enhanced infection control by CD101-expressing neutrophils was associated with increased

Fig. 5 The additional deletion of *Irfn-g* in CD101^{-/-} mice reverts severe DSS colitis. (A–C) The induction of intestinal inflammation in the indicated mouse strains was monitored by high-resolution endoscopy (A, B) and histopathological analysis of H&E-stained tissue sections (C) 10 days after DSS application. The means \pm SD of the endoscopic and histological scores from 7–9 (A) or 10–23 (B, C) individual mice are displayed, respectively. Statistical significance was calculated using one-way ANOVA with Tukey's correction ($*p \leq 0.05$; $**p < 0.01$; $***p < 0.001$). (D) The body weight of the indicated mouse strains was determined after DSS application for 10 days. Means \pm SD change in body weight (%) per group is displayed for the indicated cohorts of 6–11 animals analyzed per group. The Bonferroni *post hoc* test was used to calculate the statistical significance ($*p \leq 0.05$). (E–G) The bacterial burden in feces (E), liver (F), and spleen (G) of the indicated mouse strains was assessed by CFU plating assay and limiting dilution on day 4 following wild-type *S. Tm* infection. Each bar represents the mean \pm SD of five individual mice per group. Statistical significance was calculated using Kruskal-Wallis test ($**p < 0.01$; $***p < 0.001$). ANOVA = analysis of variance; CD = cluster of differentiation; CFU = colony forming unit; DSS = dextran sulfate sodium; IFN = interferon; *S. Tm* = *Salmonella enterica* Typhimurium; SD = standard deviation.

S.Tm infection

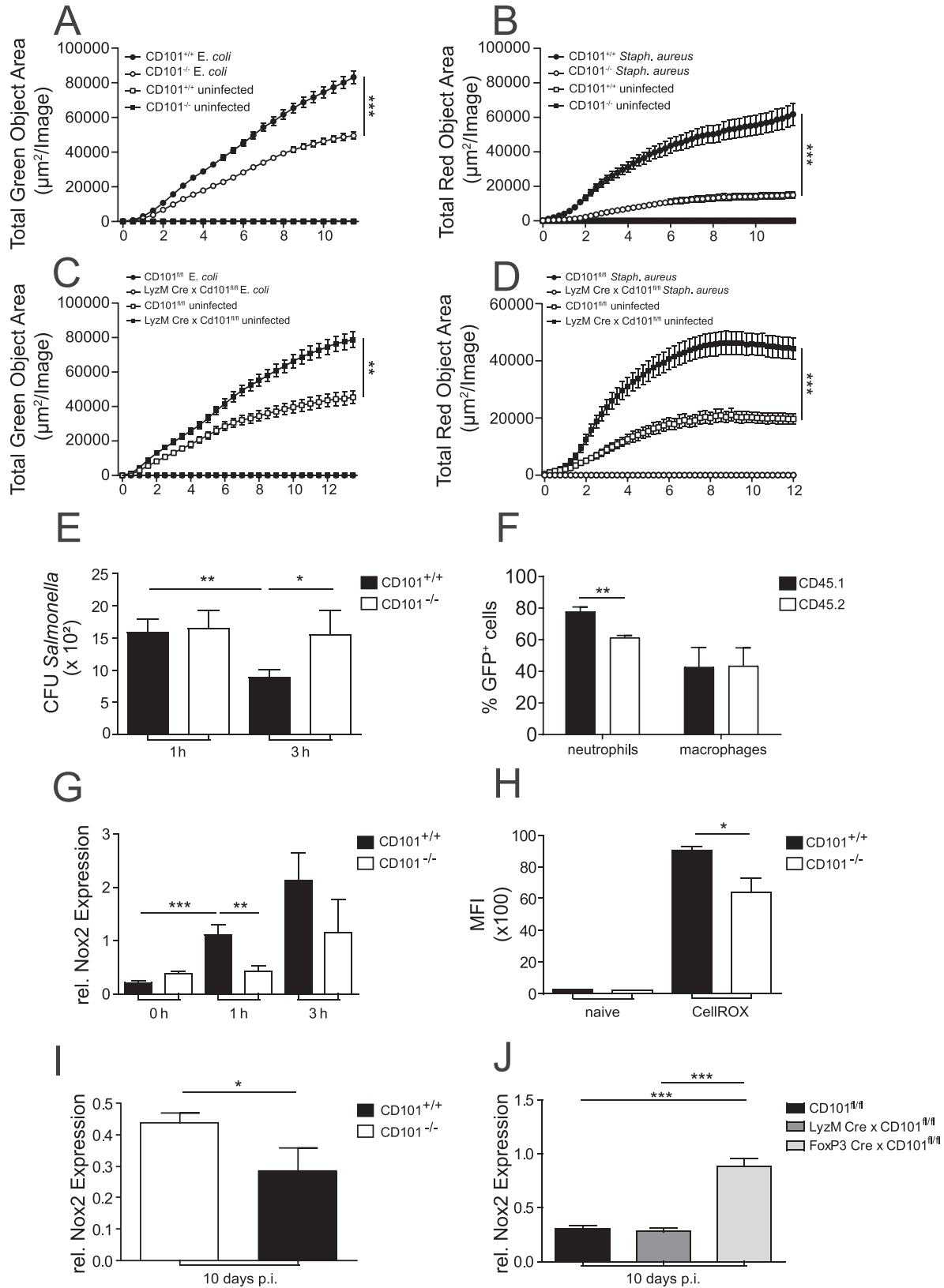


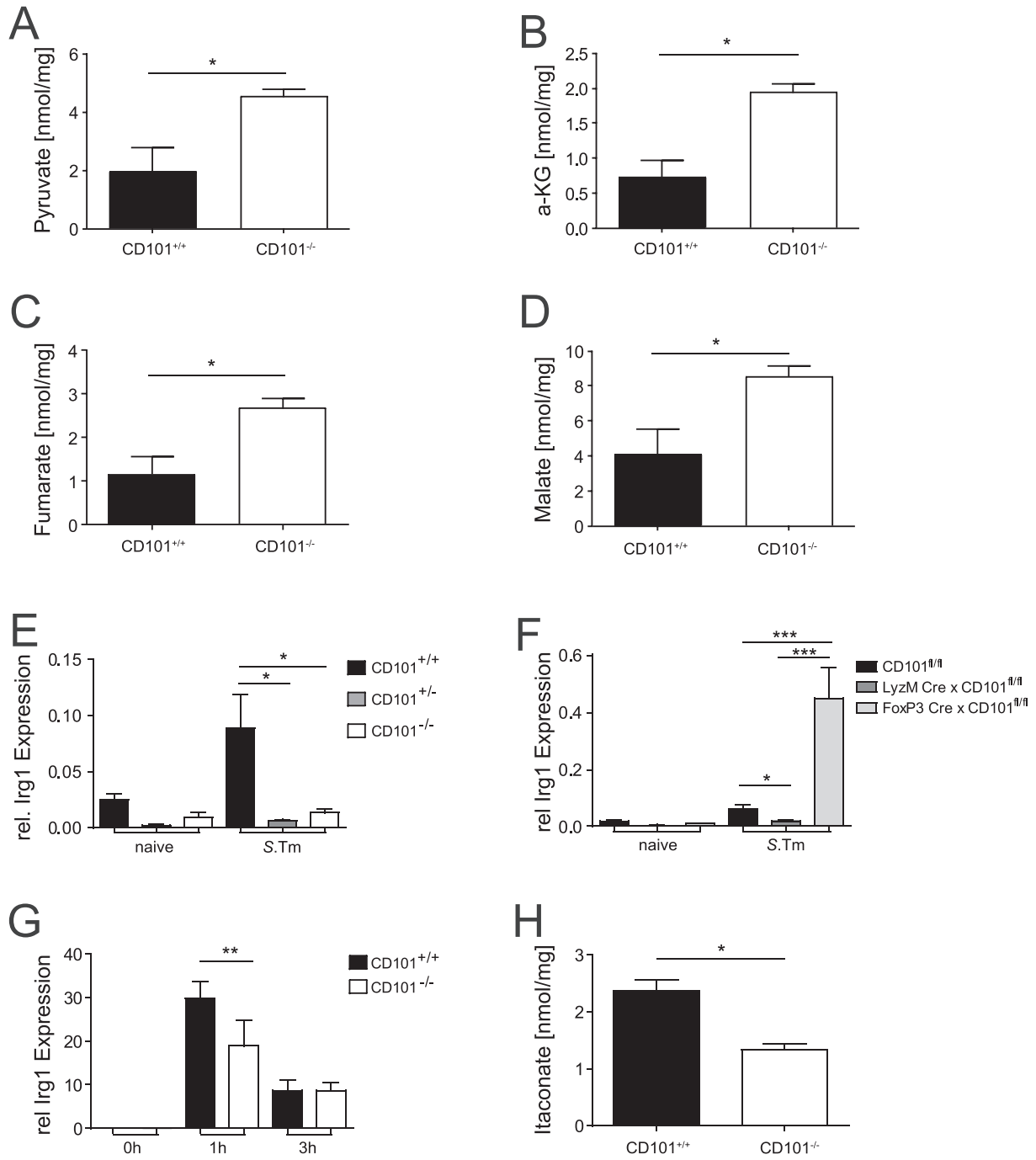
Fig. 6 CD101 expression on neutrophils is associated with an enhanced phagocytic and anti-bacterial activity of neutrophils, correlating with enhanced *Nox2* and *Irf-5* expression and an increased release of reactive oxygen species. (A–D) Relative phagocytosis shows the numbers of internalized *E. coli* (A, C) or *Staphylococcus aureus* bioparticles (B, D) relative to vehicle control in neutrophils purified from the BM of CD101^{-/-} (A, B) and *LyzM-Cre x Cd101^{fl/fl}* mice as (C, D) well as from respective wild type littermate controls. Bars show means ± SD. One-way ANOVA test with Tukey's multiple comparison test (***p* < 0.01; ****p* < 0.001). Results represent data from at least three independent experiments. (E) Intracellular bacteria were quantified in neutrophils purified from the BM of CD101^{+/+} and CD101^{-/-} mice 1 and 3 hours after infection with *S. Tm* at a MOI of 10 and relative invasion rates (1 hour) and killing rates (3 hours) were calculated. Data were compiled from four independent experiments performed in triplicates. Data were analyzed using two-way ANOVA with Tukey's *post hoc* test (**p* ≤ 0.05; ***p* < 0.01). (F) Irradiated CD45.1⁺ mice were reconstituted with a 1:1 mixture of B6 CD101^{-/-} (CD45.2⁺) and CD45.1⁺ B6 BM cells. BM chimeras were infected i.p. 6 weeks after BM reconstitution with GFP-expressing *S. Tm*. At day 1, percentages of GFP⁺ and GFP⁻ granulocytes and macrophages in the peritoneal cavities were assessed using CD45.1 allotype-specific antibodies to assign their origin to parental B6 or CD101-deficient B6 mice. Statistical significance was calculated using a linear mixed-effect model for five individual infected chimeric mice (**p* ≤ 0.05). Similar results were obtained using reciprocal BM chimeras (data not shown). (G) *Nox2* mRNA copies were determined by RT-qPCR in neutrophils purified from the BM of five CD101^{-/-} and CD101^{+/+} mice, respectively, following infection with *S. Tm* for 1 and 3 hours. The ratio of the mRNA copies of the indicated genes relative to the *Hprt* copies was calculated, and the relative increase in the respective gene copy numbers was displayed. Error bars indicate SD of the mean. Data were analyzed using two-way ANOVA with Tukey's *post hoc* test (**p* ≤ 0.05; ***p* < 0.01; ****p* < 0.001). (H) Neutrophils purified from the BM of three CD101^{-/-} mice and three respective wild-type littermate controls were analyzed for ROS release using the CellROX Deep Red Reagent (one out of three experiments). The MFI correlates with the ROS release as determined by flow cytometry. Statistical significance was calculated using a Student's *t* test for neutrophils purified from five CD101^{+/+} and CD101^{-/-} mice, respectively (**p* ≤ 0.05). (I, J) *Nox2* mRNA copies were determined by RT-qPCR in neutrophils isolated from the LP of five CD101^{-/-} (i) or seven (j) *Foxp3-Cre x CD101^{fl/fl}* or *LyzM-Cre x CD101^{fl/fl}* mice and respective controls following infection with Δ*aroA S. Tm* for 10 days. The ratio of the mRNA copies of the indicated genes relative to the *Hprt* copies was calculated, and the relative increase in the respective gene copy numbers was displayed. Data were analyzed using Kruskal-Wallis test (**p* ≤ 0.05; ****p* < 0.001). Error bars indicate SD of the mean. ANOVA = analysis of variance; BM = bone marrow; CD = cluster of differentiation; Δ*aroA S. Tm* = *S. Tm* mutant strain that lacks the *aroA* encoding 5-enolpyruvyl-3-phosphoshikimate synthetase; GFP = green fluorescent protein; i.p. = intraperitoneally; LP = lamina propria; MFI = mean fluorescent intensity; MOI = multiplicity of infection; mRNA = messenger ribonucleic acid; ROS = reactive oxygen species; RT-qPCR = reverse transcription-quantitative polymerase chain reaction; *S. Tm* = *Salmonella enterica* Typhimurium; SD = standard deviation.

availability of itaconate and ROS along with an enhanced *Irg-1* and *Nox2* expression and concomitant suppression of the TCA cycle. Importantly, CD101-mediated *Irg-1* induction promoted and sustained *Nox2* expression and activity. In conclusion, CD101 exerts immune-regulatory and anti-microbial effects, depending on the CD101-expressing cell-type tested. Therefore, CD101 appears to be not only a surface marker but also a check-point molecule for cell-specific immune functions of lymphocyte and myeloid cell subsets.

In addition to *Irg-1* and *Nox2*, *Cd101* also enhanced *Irf-5* expression. Although the expression levels of CD101 on BM-derived neutrophils are lower as compared to neutrophils purified from intestinal tissues or spleen, we obtained comparable results for the regulation of *Irg-1*, *Nox2* and *Irf-5* mRNA levels in neutrophils purified from all three tissues. In the past, IRF-5 was reported to promote neutrophil maturation and CD101 expression²³ and to impede TLR-mediated inflammatory cytokine production²⁴. While we observed reduced neutrophil num-

Fig. 7 CD101 expression on neutrophils correlates with a suppression of TCA cycle metabolites and a concomitant accumulation of itaconate. (A–D) The concentrations of pyruvate (A), α-KG (B), fumarate (C) and malate (D) were determined by hyphenated mass spectrometry in neutrophils purified from the peritoneal cavity of CD101^{+/+} and CD101^{-/-} littermates 1 day following systemic *S. Tm* infection. Data were compiled from two experiments and cells of four individual mice each. (E, F) *Irg-1* mRNA copies were determined by RT-qPCR in neutrophils purified from colonic tissues of 4–12 CD101^{-/-} mice (E), 7–10 *Foxp3-Cre x CD101^{fl/fl}* or *LyzM Cre x CD101^{fl/fl}* mice and respective controls (F) following oral infection with wild-type *S. Tm* for 4 days. (G) *Irg-1* mRNA expression in neutrophils that were isolated from the BM of six CD101^{-/-} and CD101^{+/+} littermates each, infected with *S. Tm* at a MOI of 10 *in vitro* and analyzed by RT-qPCR at the indicated time-points. The ratio of the mRNA copies of the indicated genes relative to the *Hprt* copies was calculated, and the relative increase in the respective gene copy numbers was displayed. (H) The concentration of itaconate was determined by high performance liquid chromatography (HPLC) or hyphenated mass spectrometry in neutrophils harvested from the peritoneal cavity of three CD101^{+/+} and CD101^{-/-} littermates each 1 day following systemic *S. Tm* infection. Data were analyzed using Student's *t* test (A–D, H), Kruskal-Wallis test (E, F) or two-way ANOVA with Tukey's *post hoc* test (**p* ≤ 0.05; ***p* < 0.01; ****p* < 0.001). α-KG = alpha-ketoglutarate; ANOVA = analysis of variance; BM = bone marrow; CD = cluster of differentiation; HPLC = high-performance liquid chromatography; MOI = multiplicity of infection; mRNA = messenger ribonucleic acid; RT-qPCR = reverse transcription quantitative polymerase chain reaction; *S. Tm* = *Salmonella enterica* Typhimurium; TCA = tricarboxylic acid.

S.Tm infection



bers in the BM of CD101^{-/-} mice⁸, we did not detect significant differences in *Tlr* and inflammatory cytokine expression between CD101^{+/+} and CD101^{-/-} neutrophils. In line with this observation, CD101-deficiency did not change Sca-1 expression, a marker that has been associated with an inflammatory neutrophil phenotype and impaired superoxide anion production²⁵. In contrast, CD101 expression was associated with an enhanced release of IL-10 in both models studied here, similarly as reported for the T cell transfer colitis model or genetic models of type 1 diabetes^{5,9} suggesting that CD101 mediates an anti-inflammatory phenotype rather than blocks an inflammatory one.

Several metabolic interactions exist between bacterial pathogens and immune cells of the host⁴⁹. *Irg-1* is one of the genes that inflammation and infection strongly induce³⁹. Itaconate modifies key glycolytic enzymes^{37,38} and exhibits potent anti-inflammatory and anti-microbial properties³⁵, in part due to the modulation of ROS³⁶. Importantly, neutrophils from CD101^{-/-} mice contained lower *Irg-1* and *Nox2* copy numbers and released less ROS compared to neutrophils from CD101^{+/+} litters, respectively. Moreover, *Ncf-1*^{+/-} x CD101^{-/-} mice contained substantially more *S. Tm* CFUs in their tissues compared to *Ncf-1*^{+/-} x CD101^{+/-} or *Ncf-1*^{+/+} x CD101^{+/-} littermates, and *Ncf-1*^{-/-} x CD101^{-/-} mice succumbed similarly fast as *Ncf-1*^{-/-} x CD101^{+/-} mice to *S. Tm* infections. Thus, CD101-mediated control of *Ncf-1* expression is pivotal for infection control. Moreover, our data link *Irg-1* and itaconate to CD101 in our studies and suggest that both contribute to the antimicrobial effects of CD101-expressing neutrophils, at least in part due to promoting *Nox2*. Although itaconate suppresses ulcerative colitis⁵⁰ and regulates inflammasome activation⁵¹, our studies indicate that itaconate contributed predominantly to anti-microbial rather than immunosuppressive effects, confirming its pivotal role in bacterial host defense^{33,36,52}. Moreover, neutrophils rather than other myeloid cells mediate anti-microbial effects in a CD101-dependent manner.

CD101 expression on myeloid cells in humans also sustains *Irg-1* and *Nox2*. As IBD patients exhibit lower numbers of CD101-expressing cells compared to healthy controls⁵, similarly as observed in both experimental colitis models, a disrupted CD101-dependent regulation of *Irg1* and *Nox2* in myeloid cells

might contribute to the increased susceptibility to infections observed in IBD patients^{53,54}. Indeed, missense variants of *Cd101* altering the expression of CD101 and subsequently the phenotype of immune responses^{55,56} have already been associated with an increased risk of acquiring mucosal infections⁵⁷. Moreover, CD101 might be a marker molecule for increased intestinal permeability as evidenced by the detection of more antibodies against intestinal microbial antigens in individuals expressing lower numbers of CD101-positive immune cells. Whether *Cd101* polymorphisms are associated with IBD and underlie the cell-type specific function and regulation of CD101 is subject of further investigations.

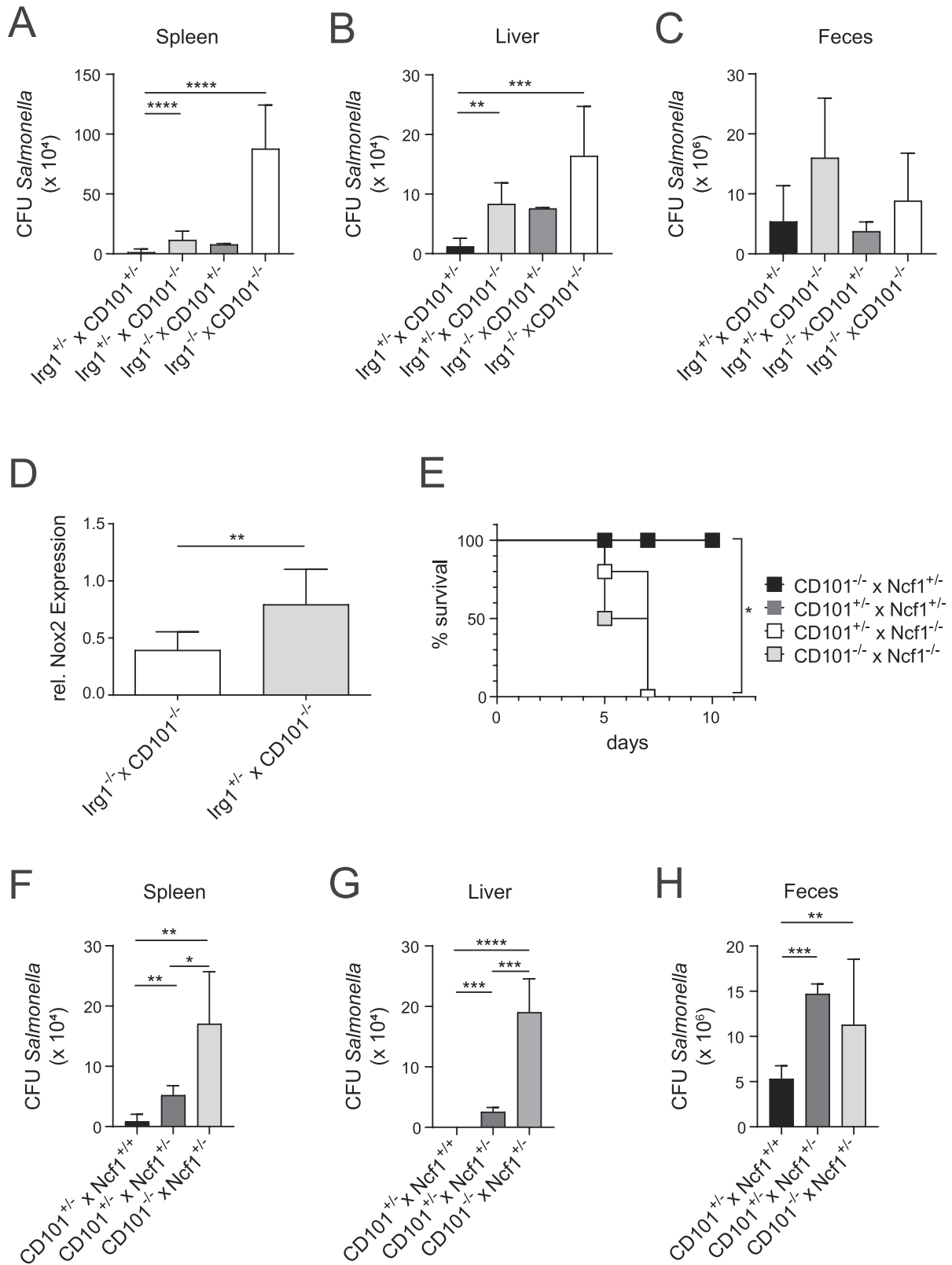
METHODS

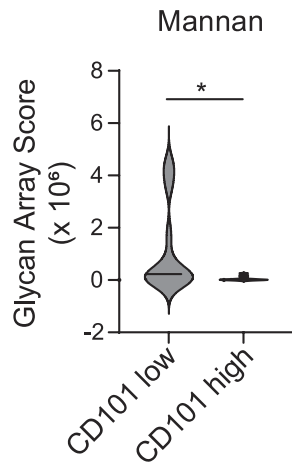
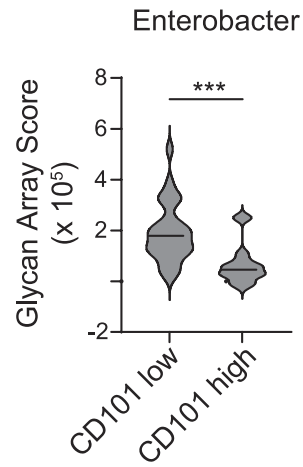
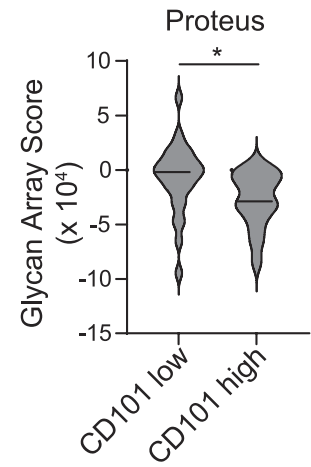
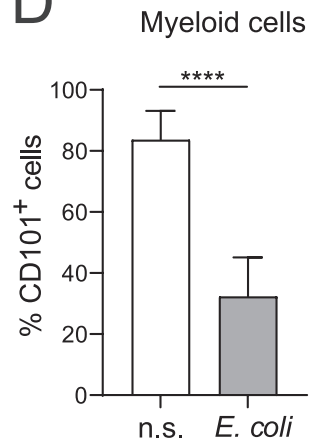
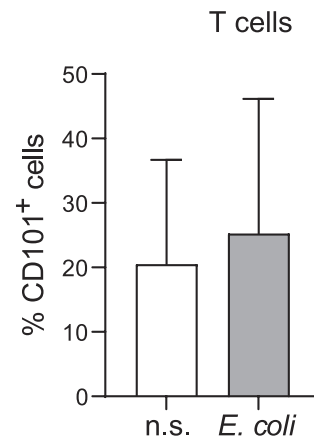
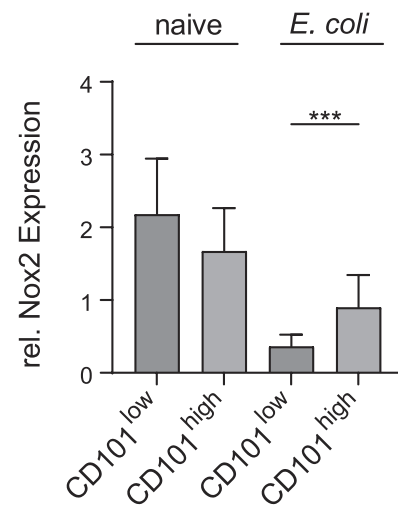
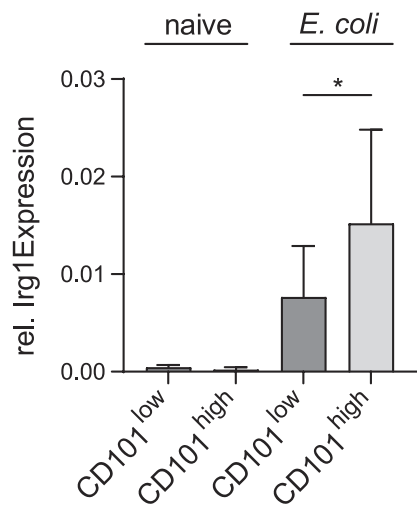
Mice

CD45.1^{+/+}, *Foxp3* Cre, *LyzM* Cre, and *Cd11c* Cre mice (all on a C57BL/6 background) were obtained from the Jackson Laboratory (Bar Harbor, ME) or from Taconic Farms (Germantown, NY, USA). Dr Markus Hoffmann kindly provided *Ncf1*^{-/-} mice, Dr Ulrike Schleicher IFN- γ ^{-/-} mice, Dr Gerhard Krönke *Cx3cr1* Cre mice, Drs. Aline Bozec and Roland Lang (all University of Erlangen-Nürnberg) IRG1^{-/-} mice and Dr Ari Waisman (University of Mainz) IL-17A/F^{-/-} mice¹⁸. The development of CD101^{-/-} and *Cd101*^{fl/fl} strains was described previously⁸. *Cd101*^{fl/fl} mice were backcrossed to *Foxp3* Cre, *LyzM* Cre, *Cd11c* Cre, or *Cx3cr1* Cre mice in order to remove the CD101 coding sequence between the two loxP sites⁸, the resulting F1 mice were crossed again to *Cd101*^{fl/fl} mice to obtain heterozygous Cre deleters and respective control mice. IFN- γ ^{-/-}, IL-17A/F^{-/-}, *Ncf1*^{-/-} and IRG1^{-/-} mice were crossed to CD101^{-/-} mice and the offspring was crossbred to obtain respective homozygous double knockout mice and respective littermate controls for more than eight generations. All mouse strains were raised in a specific pathogen-free environment. Conventional and conditional CD101-deficient mice as well as CD101^{-/-} x IL-17A/F^{-/-}, CD101^{-/-} x IFN- γ ^{-/-}, CD101^{-/-} x *Ncf-1*^{-/-}, and CD101^{-/-} x IRG1^{-/-} mice) and the respective CD101-expressing (CD101^{+/+}, CD101^{+/-} or *Cd101*^{fl/fl}) or IL-17A/F-, IFN- γ -, IRG-1- or NCF-1-expressing littermate controls were age- and sex-matched and used at 8–12 weeks of age.

Fig. 8 The CD101-mediated *Irg1* and subsequent *Nox-2* induction protects from *S. Tm* infection. (A–C) Bacterial burden in the spleens (A), livers (B), and the feces (C) of eight IRG1^{+/-} x CD101^{+/-}, six IRG1^{+/-} x CD101^{-/-}, three IRG1^{+/-} x CD101^{+/-} and six IRG1^{+/-} x CD101^{+/-} littermates was assessed by CFU plating assay and limiting dilution on day 4 following oral *S. Tm* infection. Each bar represents the mean \pm SD of the analyzed individual mice per group. Statistical significance was calculated using a two-way ANOVA (** $p < 0.01$; *** $p < 0.001$; **** $p < 0.0001$). (D) *Nox2* mRNA copies were determined by RT-qPCR in neutrophils purified from intestinal tissues of nine IRG1^{-/-} x CD101^{-/-} and nine IRG1^{+/-} x CD101^{-/-} littermates, respectively, following 1 day after infection with *S. Tm*. The ratio of the mRNA copies of the indicated genes relative to the *Hprt* copies was calculated, and the relative increase in the respective gene copy numbers is displayed. Data were analyzed using the Mann-Whitney *U* test (* $p \leq 0.05$). Error bars indicate SD of the mean. (E) Kaplan-Meier survival curves were plotted for the indicated individual mouse strains following infection with Δ aroA *S. Tm*, and statistical significance was determined by log-rank test (* $p \leq 0.05$). (F–H) Bacterial burden in the spleens (F), livers (G), and the feces (H) of four *Ncf1*^{+/+} x CD101^{+/-}, three *Ncf1*^{+/-} x CD101^{+/-} and 12 *Ncf1*^{+/-} x CD101^{-/-} littermates was assessed by CFU plating assay and limiting dilution on day 10 following oral *S. Tm* infection with the Δ aroA mutant. Each bar represents the mean \pm SD of the analyzed individual mice per group. Statistical significance was calculated using a two-way ANOVA (* $p \leq 0.05$; ** $p < 0.01$; *** $p < 0.001$; **** $p < 0.0001$). ANOVA = analysis of variance; CD = cluster of differentiation; CFU = colony-forming unit; Δ aroA = *S. Tm* mutant strain that lacks the *aroA* encoding 5-enolpyruvyl-3-phosphoshikimate synthetase; mRNA = messenger ribonucleic acid; RT-qPCR = reverse transcription-quantitative polymerase chain reaction; *S. Tm* = *Salmonella enterica* Typhimurium; SD = standard deviation.

S.Tm infection



A**B****C****D****E****F****G**

Infection with *Salmonella Typhimurium* (*S. Tm*)

The *S. Tm* wild-type strain SL1344 and the *S. Tm* mutant strain Δ aroA¹⁴ were grown in LB broth containing 100 μ g/mL streptomycin (Sigma-Aldrich, Darmstadt, Germany). Dr Roman Gerlach kindly provided GFP-expressing *S. Tm*. CFUs of *S. Tm* in the exponential growth phase were determined at OD₆₀₀. All mice in the respective experiments received 20 mg/kg bodyweight streptomycin orally 5–12 hours prior to infection with 1×10^6 CFUs of Δ aroA or wild-type *S. Tm* in 100 μ L PBS (pH 7.4) by oral gavage¹³. To study systemic infections, the respective mouse strains were infected i.p. with 1×10^2 CFUs of wild-type *S. Tm*.

DSS colitis

To induce acute DSS colitis in mice, 2.0%–2.5% DSS (40 kDa; MP Biomedicals, Eschwege, Germany) was added to the drinking water for 7 days, followed by normal drinking water until day 10. For the induction of chronic colitis, 1.5%–2.0% DSS was applied in three consecutive 7-day cycles with 2-week intervals of drinking water. Knockouts and littermates were separated 2–3 weeks before the start of the experiments.

Statistical analysis

Samples were analyzed for normal distribution by a Kolmogorov-Smirnov test. According to the results, statistical significance in normal distributed samples was analyzed by one-way analysis of variance with *post hoc* test (Bonferroni) and Student's *t* test, and samples failing the normal distribution test by Kruskal-Wallis test with *post hoc* (Dunn's multiple comparison) or Mann-Whitney *U* test as indicated in the respective experiments. A sample size of at least three ($n = 3$) was used for each sample group in a given experiment, and a *p* value of 5% ($*p \leq 0.05$), 1% ($**p \leq 0.01$), or 0.1% ($***p \leq 0.001$) was considered significant to accept the alternate hypothesis. GraphPad Prism software (San Diego, CA) was used for statistical analysis.

Study approval

All procedures were approved by the local ethics committee of FAU Erlangen-Nürnberg. Patients gave written informed consent before participation in the study. All animal studies were performed in accordance with German law and approved by the Institutional Animal Care and Use Committee of FAU Erlangen-Nürnberg and the Animal Experiment Committee of the State Government of Lower Franconia, Würzburg, Germany.

DECLARATION OF COMPETING INTEREST

The authors have declared that no conflict of interest exists.

CREDIT AUTHORSHIP CONTRIBUTION STATEMENT

Marius Wrage: Methodology, Investigation, Formal analysis, Data curation. **Tim Holland:** Visualization, Methodology, Investigation, Formal analysis. **Björn Nüse:** Methodology, Investigation, Formal analysis, Data curation. **Johanna Kaltwasser:** Methodology, Investigation, Formal analysis. **Jessica Fröhlich:** Methodology, Investigation, Formal analysis. **Harald Arnold:** Methodology, Investigation. **Claudia Gießler:** Methodology, Investigation. **Cindy Flamann:** Methodology, Investigation, Formal analysis. **Heiko Bruns:** Writing – review & editing. **Johannes Berges:** Methodology, Investigation, Formal analysis. **Christoph Daniel:** Methodology, Investigation, Formal analysis, Data curation. **Markus H. Hoffmann:** Writing – review & editing, Methodology, Investigation, Formal analysis, Data curation. **Chakkumkal Anish:** Methodology, Investigation, Formal analysis, Data curation. **Peter H. Seeberger:** Writing – review & editing. **Christian Bogdan:** Writing – review & editing. **Katja Dettmer:** Methodology, Investigation, Formal analysis, Data curation. **Manfred Rauh:** Writing – review & editing, Methodology, Investigation, Formal analysis, Data curation. **Jochen Mattner:** Writing – review & editing, Writing – original draft, Supervision, Project administration, Funding acquisition, Conceptualization.

ACKNOWLEDGMENTS

We thank Adson Arnold, Julia Baier, Martin Purtak, and Regina Schey for technical assistance and Prof. Raja Atreya as well as all medical personnel of the Department of Medicine I at the University Hospital Erlangen for collecting human blood and serum samples for our studies. The German Research Foundation (DFG-CRC1181-project number C04, DFG-MA 2621/4-1 and DFG-MA 2621/5-1 and GRK2740), the Sino German Center Mobility Programme (M-693), the Staedtler Stiftung (23/14), the Johannes and Frieda Marohn Stiftung (Alz/Iko – Matt/2022) and the Max Planck Society supported this study.

APPENDIX A. SUPPLEMENTARY MATERIAL

Supplementary material to this article can be found online at <https://doi.org/10.1016/j.mucimm.2024.06.004>.

Fig. 9 An enhanced systemic reactivity to bacterial antigens correlates with a reduced CD101 expression on myeloid cells in IBD patients. (A–C) Detection of immunoglobulin (Ig)G antibodies to fungal mannan (A) or *Enterobacter* (B) and *Proteus* (C) oligosaccharides in serum samples of IBD patients. IBD patients were separated into CD101^{low} and CD101^{high} expressing cohorts, based on the expression of CD101 on myeloid cells. The reactivity of the respective sera to the indicated antigens was determined by microarray scans. Each symbol represents an individual patient. (D+E) The distribution of CD101-expressing myeloid cells (D) and T lymphocytes (E) was determined in 12 individual healthy donors by flow cytometry before and after stimulation with heat-killed *E. coli*. Statistical significance in panels a–e was assessed using Student's *t* test ($*p \leq 0.05$; $***p \leq 0.001$; $****p < 0.0001$). (F+G) *Nox2* (F) and *Irg-1* (G) mRNA copies were determined by RT-qPCR in myeloid cells of CD101^{low} and CD101^{high} expressing donor cohorts before and after stimulation with heat-killed *E. coli* antigens. The ratio of the mRNA copies of the indicated genes relative to the *Gapdh* is displayed. Data were analyzed using Kruskal-Wallis test ($*p \leq 0.05$; $***p \leq 0.001$). Error bars indicate SD of the mean. CD = cluster of differentiation; IBD = inflammatory bowel disease; Ig = immunoglobulin; mRNA = messenger ribonucleic acid; RT-qPCR = reverse transcription-quantitative polymerase chain reaction; SD = standard deviation.

References

1. Rioux, J. D. & Abbas, A. K. Paths to understanding the genetic basis of autoimmune disease. *Nature* **435**, 584–589 (2005).
2. Walker, L. S. K. & Abbas, A. K. The enemy within: keeping self-reactive T cells at bay in the periphery. *Nat. Rev. Immunol.* **2**, 11–19 (2002).
3. Bach, J. F. The hygiene hypothesis in autoimmunity: the role of pathogens and commensals. *Nat. Rev. Immunol.* **18**, 105–120 (2018).
4. Abraham, C. & Cho, J. H. Inflammatory bowel disease. *N. Engl. J. Med.* **361**, 2066–2078 (2009).
5. Schey, R. et al. CD101 inhibits the expansion of colitogenic T cells. *Mucosal Immunol.* **9**, 1205–1217 (2016).
6. Mohammed, J. P. et al. Identification of CD101 as a susceptibility gene for *Novosphingobium aromaticivorans*-induced liver autoimmunity. *J. Immunol.* **187**, 337–349 (2011).
7. Ruegg, C. L. et al. V7, a novel leukocyte surface protein that participates in T cell activation. II. Molecular cloning and characterization of the V7 gene. *J. Immunol.* **154**, 4434–4443 (1995).
8. Rainbow, D. B. et al. Evidence that CD101 is an autoimmune diabetes gene in nonobese diabetic mice. *J. Immunol.* **187**, 325–336 (2011).
9. Mattner, J. et al. Genetic and functional data identifying CD101 as a type 1 diabetes (T1D) susceptibility gene in nonobese diabetic (NOD) mice. *PLoS Genet.* **15**:e1008178.
10. Wrage, M., Kaltwasser, J., Menge, S. & Mattner, J. CD101 as an indicator molecule for pathological changes at the interface of host-microbiota interactions. *Int. J. Med. Microbiol.* **311**:151497.
11. Zeng, R., Bscheider, M., Lahl, K., Lee, M. & Butcher, E. C. Generation and transcriptional programming of intestinal dendritic cells: essential role of retinoic acid. *Mucosal Immunol.* **9**, 183–193 (2016).
12. Okayasu, I. et al. A novel method in the induction of reliable experimental acute and chronic ulcerative colitis in mice. *Gastroenterology* **98**, 694–702 (1990).
13. Barthel, M. et al. Pretreatment of mice with streptomycin provides a *Salmonella enterica* serovar Typhimurium colitis model that allows analysis of both pathogen and host. *Infect. Immun.* **71**, 2839–2858 (2003).
14. Grassl, G. A., Valdez, Y., Bergstrom, K. S. B., Vallance, B. A. & Finlay, B. B. Chronic enteric salmonella infection in mice leads to severe and persistent intestinal fibrosis. *Gastroenterology* **134**, 768–780 (2008).
15. Evrard, M. et al. Developmental analysis of bone marrow neutrophils reveals populations specialized in expansion, trafficking, and effector functions. *Immunity* **48**, 364–379.e8 (2018).
16. Kühn, R., Löhler, J., Rennick, D., Rajewsky, K. & Müller, W. Interleukin-10-deficient mice develop chronic enterocolitis. *Cell* **75**, 263–274 (1993).
17. Spencer, S. D. et al. The orphan receptor CRF2-4 is an essential subunit of the interleukin 10 receptor. *J. Exp. Med.* **187**, 571–578 (1998).
18. Haas, J. D. et al. Development of interleukin-17-producing $\gamma\delta$ T cells is restricted to a functional embryonic wave. *Immunity* **37**, 48–59 (2012).
19. Tang, C. et al. Suppression of IL-17F, but not of IL-17A, provides protection against colitis by inducing Treg cells through modification of the intestinal microbiota. *Nat. Immunol.* **19**, 755–765 (2018).
20. Keestra, A. M. et al. Early MyD88-dependent induction of interleukin-17A expression during *Salmonella colitis*. *Infect. Immun.* **79**, 3131–3140 (2011).
21. Songhet, P. et al. IL-17A/F-signaling does not contribute to the initial phase of mucosal inflammation triggered by *S. Typhimurium*. *PLoS One* **5**:e13804.
22. Bogdan, C. Nitric oxide synthase in innate and adaptive immunity: an update. *Trends Immunol.* **36**, 161–178 (2015).
23. Khoyratty, T. E. et al. Distinct transcription factor networks control neutrophil-driven inflammation. *Nat. Immunol.* **22**, 1093–1106 (2021).
24. Bellissimo, D. C. et al. Runx1 negatively regulates inflammatory cytokine production by neutrophils in response to toll-like receptor signaling. *Blood Adv.* **4**, 1145–1158 (2020).
25. Park, M. Y., Kim, H. S., Lee, H. Y., Zabel, B. A. & Bae, Y. S. Novel CD11b⁺Gr-1⁺Sca-1⁺ myeloid cells drive mortality in bacterial infection. *Sci. Adv.* **6**:eaax8820.
26. Winterbourn, C. C., Kettle, A. J. & Hampton, M. B. Reactive oxygen species and neutrophil function. *Annu. Rev. Biochem.* **85**, 765–792 (2016).
27. Chandel, N. S. NADPH—the forgotten reducing equivalent. *Cold Spring Harb. Perspect. Biol.* **13**.
28. Ganeshan, K. & Chawla, A. Metabolic regulation of immune responses. *Annu. Rev. Immunol.* **32**, 609–634 (2014).
29. Williams, N. C. & O'Neill, L. A. J. A role for the Krebs cycle intermediate citrate in metabolic reprogramming in innate immunity and inflammation. *Front. Immunol.* **9**, 141 (2018).
30. Tannahill, G. M. et al. Succinate is an inflammatory signal that induces IL-1 β through HIF-1 α . *Nature* **496**, 238–242 (2013).
31. Rosenberg, G. et al. Host succinate is an activation signal for *Salmonella* virulence during intracellular infection. *Science* **371**, 400–405 (2021).
32. Martínez-Reyes, I. & Chandel, N. S. Mitochondrial TCA cycle metabolites control physiology and disease. *Nat. Commun.* **11**, 102 (2020).
33. Michelucci, A. et al. Immune-responsive gene 1 protein links metabolism to immunity by catalyzing itaconic acid production. *Proc. Natl Acad. Sci. U. S. A.* **110**, 7820–7825 (2013).
34. Bambouskova, M. et al. Electrophilic properties of itaconate and derivatives regulate the I κ B ζ -ATF3 inflammatory axis. *Nature* **556**, 501–504 (2018).
35. O'Neill, L. A. J. & Artyomov, M. N. Itaconate: the poster child of metabolic reprogramming in macrophage function. *Nat. Rev. Immunol.* **19**, 273–281 (2019).
36. Hall, C. J. et al. Immuno-responsive gene 1 augments bactericidal activity of macrophage-lineage cells by regulating beta-oxidation-dependent mitochondrial ROS production. *Cell Metab.* **18**, 265–278 (2013).
37. Qin, W. et al. S-glycosylation-based cysteine profiling reveals regulation of glycolysis by itaconate. *Nat. Chem. Biol.* **15**, 983–991 (2019).
38. Liao, S. T. et al. 4-octyl itaconate inhibits aerobic glycolysis by targeting GAPDH to exert anti-inflammatory effects. *Nat. Commun.* **10**, 5091 (2019).
39. Tallam, A. et al. Gene regulatory network inference of Immuno-responsive gene 1 (IRG1) identifies interferon regulatory factor 1 (IRF1) as its transcriptional regulator in mammalian macrophages. *PLoS One* **11**, e0149050 (2016).
40. Wu, R., Chen, F., Wang, N., Tang, D. & Kang, R. ACOD1 in immunometabolism and disease. *Cell Mol. Immunol.* **17**, 822–833 (2020).
41. Lambeth, J. D. NOX enzymes and the biology of reactive oxygen. *Nat. Rev. Immunol.* **4**, 181–189 (2004).
42. Van Acker, H. & Coenye, T. The role of reactive oxygen species in antibiotic-mediated killing of bacteria. *Trends Microbiol.* **25**, 456–466 (2017).
43. McKenzie, S. J., Baker, M. S., Buffinton, G. D. & Doe, W. F. Evidence of oxidant-induced injury to epithelial cells during inflammatory bowel disease. *J. Clin. Invest.* **98**, 136–141 (1996).
44. Ramonaite, R. et al. Influence of NADPH oxidase on inflammatory response in primary intestinal epithelial cells in patients with ulcerative colitis. *BMC Gastroenterol.* **13**, 159 (2013).
45. Yokota, H. et al. NOX1/NADPH oxidase expressed in colonic macrophages contributes to the pathogenesis of colonic inflammation in trinitrobenzene sulfonic acid-induced murine colitis. *J. Pharmacol. Exp. Ther.* **360**, 192–200 (2017).
46. Pizzolla, A. et al. Reactive oxygen species produced by the NADPH oxidase 2 complex in monocytes protect mice from bacterial infections. *J. Immunol.* **188**, 5003–5011 (2012).
47. Mehandru, S. & Colombel, J. F. The intestinal barrier, an arbitrator turned provocateur in IBD. *Nat. Rev. Gastroenterol. Hepatol.* **18**, 83–84 (2021).
48. Geissner, A. et al. Microbe-focused glycan array screening platform. *Proc. Natl Acad. Sci. U. S. A.* **116**, 1958–1967 (2019).
49. Traven, A. & Naderer, T. Central metabolic interactions of immune cells and microbes: prospects for defeating infections. *EMBO Rep.* **20**:e47995.
50. Wang, Q. et al. The anti-inflammatory drug dimethyl itaconate protects against colitis-associated colorectal cancer. *J. Mol. Med. (Berl.)* **98**, 1457–1466 (2020).
51. Hoofman, A. et al. The immunomodulatory metabolite itaconate modifies NLRP3 and inhibits inflammasome activation. *Cell Metab.* **32**, 468–478.e7 (2020).
52. Chen, M. et al. Itaconate is an effector of a Rab GTPase cell-autonomous host defense pathway against *Salmonella*. *Science* **369**, 450–455 (2020).
53. Singh, S., Facciorusso, A., Dulai, P. S., Jairath, V. & Sandborn, W. J. Comparative risk of serious infections with biologic and/or immunosuppressive therapy in patients with inflammatory bowel diseases: a systematic review and meta-analysis. *Clin. Gastroenterol. Hepatol.* **18**, 69–81.e3 (2020).
54. Long, M. D., Martin, C., Sandler, R. S. & Kappelman, M. D. Increased risk of pneumonia among patients with inflammatory bowel disease. *Am. J. Gastroenterol.* **108**, 240–248 (2013).
55. Okuno, M. et al. Nucleotide substitutions in CD101, the human homolog of a diabetes susceptibility gene in non-obese diabetic mouse, in patients with type 1 diabetes. *J. Diabetes Investig.* **8**, 286–294 (2017).
56. Richert-Spuhler, L. E. et al. CD101 genetic variants modify regulatory and conventional T cell phenotypes and functions. *Cell Rep. Med.* **2**:100322.
57. Mackelprang, R. D. et al. Whole genome sequencing of extreme phenotypes identifies variants in CD101 and UBE2V1 associated with increased risk of sexually acquired HIV-1. *PLoS Pathog.* **13**:e1006703.